DRAG ON CYLINDERS IN NON-NEWTONIAN FLUIDS

A Thesis Submitted

In Partial Fulfillment of the Requirements

For the Degree of

MASTER OF TECHNOLOGY

by

Chandan Kumar Jena

To the

DEPARTMENT OF CHEMICAL ENGINEERING

INDIAN INSTITUTE OF TECHNOLOGY, KANPUR

FEBRUARY, 2001

CERTIFICATE

It is certified that the work presented in this thesis entitled **Drag on Cylinders in Non-Newtonian Fluids** has been carried out by **Mr. Chandan Kumar Jena** under my supervision and that this work has not been submitted elsewhere for the award of a degree.

February 2001.

Dr. R.P. Chhabra
Professor,
Department of Chemical Engineering
Indian Institute of Technology Kanpur, 208016

DEDICATED

TO MY PARENTS

Sometimes I Forget To Say
How Much I Love U

Acknowledgements

I wish to express my sincere and heartful thanks to my thesis supervisor, Dr. R.P.Chhabra whose excellent guidance, affectionate encouragement and inspiration with all-round cooperation have enabled me to bring the work to the present form. It was indeed a real pleasure and great privilege to have been associated with him.

Special thanks to my friends Deepak, Mandhani, Rajat, Vajpayee, Jayram, Sharma, Jitu, Gopal, Anoop, Anil and Subodh for their help during my thesis work.

I wish to extend my thanks to all my friends Santosh Dehury, Gopal, Santosh Rout, Biswal, Sanjay, Mahalik, Himansu, Saswat and others for their memorable company through out my stay at IIT Kanpur.

I am extremely thankful to the almighty for gifting me such a nice and dedicated parents whose great sacrifice, affection, benevolence and constant moral support without which my life is meaning less.

Chandan kumar Jena

Contents

Appendices

Abstract

The effect of confining walls and shape and orientation on the free settling behavior of cylindrical particles in Newtonian and non-Newtonian fluids has been investigated. Cylinders having wide length-to-diameter ratio (0.25 to 48.3) have been used in this work. The terminal velocity was measured as a function of the physical properties of a series of test fluids. Furthermore, the retardation effect exerted by the confining boundaries on the free settling velocity has been quantified by performing experimental measurements in five different sizes of rectangular fall vessels. The experiments were carried out for vertical and horizontal orientations of cylindrical particles. The raw experimental data on terminal velocity has been converted into useful dimensionless variables. Based on these data for Newtonian and non-Newtonian fluids, simple empirical correlations on wall effects have been presented. The drag results were calculated from these data and were compared with the existing correlations. The present investigation encompasses the following ranges of conditions:

Newtonian fluids:

$0.013 < Re < 1.2$

Non-Newtonian fluids:

$10^{-5} < Re < 0.55$

List of Figures

List of Tables

Chapter 1

Introduction

The translational motion of a cylindrical particle in Newtonian and non-Newtonian solutions is a problem of practical interest. Non-Newtonian fluid behavior is encountered in an overwhelming number of situations throughout the nature and in commercial operations. Typical examples of materials exhibiting non-Newtonian flow characteristics include multiphase mixtures (slurries, emulsions, gas-liquid dispersions), polymer melts and solutions, biological fluids (blood, saliva, synovial fluid, etc) and agricultural and diary wastes, etc. Other examples of importance include the enhanced recovery of oil from oil shale, industrial waste flow process, slurry operations, polymer and plastic synthesis and fabrication, food processing and biological processing, etc. Due to such widespread applications, considerable work has been devoted towards the understanding of the flow behavior of non-Newtonian fluids in a range of hydrodynamic situations.

One important class of problems involves the motion of particles in quiescent fluid media. So a knowledge of the terminal settling velocity of particles in quiescent fluids, and the drag force on the particles placed in moving fluid streams is often required in a wide ranging applications in chemical, mineral and process industries. Typical examples include process design calculations for continuous asceptic processing of large food particles, fixed and fluidized bed reactors, pneumatic and hydraulic conveying of coarse particles, liquid-solid separation and classification techniques, etc. So the flow of fluids past a non-spherical particle like cylinder represents an idealization of many industrially important processes. Important examples include the processing of fiber suspensions, catalytic reactors employing catalyst in the form of cylindrical pellets, etc. In all these applications, the quantity of central interest is the free fall velocity of a cylinder falling under the influence of gravity which is strongly influenced by the orientation, presence of finite boundaries and the rheological properties of the fluids, or

conversely, the drag force exerted by a moving liquid stream on an object held stationary. In contrast to the vast literature available on the motion of spherical particles falling in different geometrical vessels, much less is known about the settling characteristics of particles of cylindrical shape.

As mentioned earlier, the motion of particles through fluids at low Reynolds number is appreciably affected by the container walls. Again the flow characteristics are a function of the geometry of the wall. The steady motion of particles through unbounded fluids has been a subject of theoretical interest for many years. Experimentally, however, it is impractical to approach the unbounded condition, so many reported studies, both theoretical and experimental, have been concerned with the effect of finite boundaries on the settling velocity of a freely falling particle. The orientation of the cylindrical particle affects the settling characteristics to a greater extent. A very few studies are available on the flow behavior of cylindrical particles of finite aspect ratios in Newtonian and non-Newtonian fluids where orientation is one of the significant parameters.

1.1 Scope of the present work

In particular, the objectives of this work are tc determine the drag coefficient for non-spherical particles, especially cylindrical particles of varying aspect ratios (0.25 to 48.3) moving with their axes parallel and normal to the direction of motion in Newtonian and non-Newtonian solutions, and to ascertain the influence of the rectangular walls on the settling characteristics.

Chapter 2

Literature Review

As mentioned earlier, numerous theoretical and experimental analyses relate to axisymmetric shapes and to the conditions when the particle Reynolds number is small and with different geometry of the settling vessels. In this chapter, a brief account of the previous studies on the free settling behavior of regular but non-spherical shaped particles like cylinders, rectangular prisms, cones, etc in Newtonian and non-Newtonian fluids is presented which in turn facilitates the setting out of the objectives of this work.

2.1 Newtonian Media

Considerable amount of work is available on all aspects of sphere motion in incompressible Newtonian media and consequently, a wealth of information is now available on the macroscopic as well as microscopic fluid flow phenomena in this flow configuration. For the past century Stokes law (1851) for a sphere falling freely in a viscous fluid has been well accepted. Perry (1941) lists many investigators whose combined experimental data verify the validity of the Stokes law at low Reynolds numbers. Most of the developments in this area up to 1978 are summarized in the classic book by Clift *et al.*(1978). Other sources of information include Happel and Brenner (1965) and Hetsroni (1982).

In contrast, however, the analogous studies involving non-spherical particles have been less extensive. Overbeck (1876) developed an integral equation for an ellipsoid from which its resistance to motion in a viscous fluid is made equal to that of a sphere. Since Overbeck's general equation for the resistance of an ellipsoid is difficult to integrate when all the semi-axes are of different values, Gans (1911) simplified the resistance equation by assuming an ellipsoid of revolution (spheroid). He proved analytically that a body possessing three perpendicular symmetry planes has no tendency

to assume any particular orientation as it settles in a viscous fluid. The resistance equations for very thin discs, settling edgewise and broad wise in a viscous fluid, have been derived from the general, analytical equation for a ellipsoid, developed by Overbeck (1876). The case of viscous motion transverse to a long elliptic cylinder has been treated analytically by Bairstow (1923), using the linearized equation of Overbeck (1876) as a basis in the investigation.

It is readily recognized that the drag force experienced by an object settling in a quiescent viscous medium is strongly influenced by the shape and orientation of the body apart from the usual variables such as its size, density, and the density and viscosity of the liquid. For instance, depending upon the values of the Reynolds number and of the length to diameter ratio, a cylinder may fall with its axis normal or parallel to the direction of motion. Theoretical treatments have generally been limited to the creeping motion of axisymmetric bodies such as oblate and prolate spheroids, discs or slender bodies such as cylinders and needles. Analytical expressions for the relevant stream function and drag coefficient are available in the literature (Happel and Brenner,1965; Clift *et al.* 1978;Kim and Karrila,1991). Limited results for the settling of spheroids outside the creeping flow regimes are also available (Masliyah and Epstein, 1970). Analogous analysis for cylinders, rectangular prisms, cones etc. is available in the works of Unnikrishnan and Chhabra (1990), Sharma and Chhabra (1991), and Venumadhav and Chhabra (1994). The theoretical studies of the extent of wall effects and drag for a thin disc in the low Reynolds number regime are available in the literature (Overbeck, 1876; Shail and Norton, 1969). Aside from these analytical studies, very few experimental results are available on the terminal velocities of circular discs in Newtonian media (Schiemedel, 1928; Squires and Squires, 1937; Chhabra *et al.*, 1996). In most of the aforementioned studies particles were settled with one orientation, except in a few, which are again limited to the streamline region.

The first experimental study of the effect of orientation on the settling rate of non-isometric particles was made by Squires and Squires (1937). Using blended mineral oils, they settled very thin, almunium discs, ranging in thickness to diameter ratio of 0.00062 to 0.0063, in edge-wise and broad-wise orientation. Their correlation related the drag coefficient to the Reynolds number by a single curve for both orientations. Similar

studies have been reported by Kunkel (1948). Wieselsberger (1922) conducted experiments in the turbulent region with thin discs of various diameters and cylinders with a length to diameter ratio of five. Heiss and Coull (1952) reported extensive work by treating their experimental data by empirical methods for both horizontal (round-wise) and vertical (flat-wise) motion of cylinders, rectangular parallelepipeds and spheroids.

Currently there are two approaches available to represent and correlate the terminal settling data for non-spherical objects. In the first approach, the usual drag coefficient-Reynolds number form is used. The works of Finn (1953), Jones and Knudsen (1961), List and Schmenauer (1971), Kasper *et al.* (1985), Unnikrishnan and Chhabra (1990) and Sharma and Chhabra (1991), etc. illustrate the applicability of this approach. Much confusion, however, exists regarding the choice of a suitable linear dimension. Some investigators have found the use of a volume equivalent sphere diameter satisfactory (Heiss and Coull, 1952; Leith, 1987; Sharma and Chhabra, 1991; Venumadhav and Chhabra, 1994). While others have advocated the use of a shape factor together with an equivalent volume sphere diameter (Pettyjohn and Christiansen, 1948; McNown and Malaika,1950; Swamee and Ojha, 1991). Yet others have employed an equivalent diameter based on equal surface areas. Kasper (1982) has written an interesting article on the relative merits and demerits of a variety of equivalent diameters and shape factors currently used in correlating the drag coefficient data. Irrespective of the choice of a suitable equivalent diameter (whether in conjuction with a shape factor or not), this approach endeavors to reconcile the drag coefficient data for variously shaped particles into one curve, akin to the standard drag curve for spheres. Sometimes, additional geometric factors such as the aspect ratio in case of cylinders also appear in the final drag expressions.

In the other approach, the terminal velocity measurements are presented and correlated in terms of a velocity ratio. In essence, this approach denotes the behavior of a non-spherical particle in comparison with that of an equivalent sphere of the same volume and other geometric ratios. This approach introduces a sphericity factor, ψ, which is defined as the ratio of the surface area of a sphere (of the same volume) to that of the actual particle. Another nominal diameter, d_n, is introduced which is defined as the diameter of a circle having an area equal to the projected area of the particle in a direction

normal to that of flow. Finally, one defines a factor, K_v, which is the ratio of the settling velocity of a non-spherical particle to that of a sphere of the same volume. This approach has been used , for instance, by Pettyjohn and Christiansen (1948), Heiss and Coull (1952), McNown and Malaika (1950), Singh and Roychoudhury (1969) and more recently by Unnikrishnan and Chhabra (1990), Venu Madhav and Chhabra (1994). Though this approach also proved to be quite successful for correlating the experimental results for variously shaped particles in Newtonian fluids but a universal correlation encompassing all shapes of interest under wide conditions is yet to emerge.

Depending upon the aspect ratio and the geometrical shape of the boundary, the confining walls exert additional retardation force on the moving body. Thus to estimate the net fluid dynamic drag, a wall correction is needed. This is accomplished by introducing a wall factor 'f ', which is defined as the ratio of the measured velocity in a bounded medium to that in an unbounded medium. Thus the value of the wall factor ranges from zero to one. Again, while extensive literature is now available on the wall effects to sphere motion in cylindrical and non-circular geometries (eg. See Clift *et al.*, 1978; Chhabra,1993), much less is known about the extent of wall effects on the free settling motion of non-spherical objects. Some investigators have ignored the wall effects while others have applied the same correction as for spheres (McNown and Malaika, 1950; Willmarth *et al.*, 1964; Jayaweera and Cottis, 1969; Roos and Willmarth, 1971; Johnson *et al.*,1987). Clearly, neither of these procedures is justifiable. Kasper (1987) has clearly shown the importance of wall effects on the creeping motion of arbitrary shaped particles. Indeed, the wall effects are believed to be as significant in the case of non-spherical particles as that for spheres. For instance, the aspect ratio (sphere/cylinder diameter) of 0.1 causes 21% reduction in the free settling velocity at low Reynolds numbers. Only, Unnikrishnan and Chhabra (1991), Sharma and Chhabra (1991), and Venumadhav and Chhabra (1994) have corrected their experimental data for wall effects.

Again, there has been very little work on the hydrodynamic behavior of particles settling in the presence of non-circular walls such as triangular, rectangular, square etc. De Mestre (1973) has experimented with slender cylinders near a single plane wall and in between two parallel plane walls and compared the drag coefficients with the theoretical values. Happel and Bart (1974) have theoretically investigated the settling of a sphere

along the axis of a long square duct filled with an incompressible Newtonian medium. Their analysis elucidates the extent of the retardation effect on the sphere exerted by the square confining walls when the aspect ratio is small (R/L<0.1). The magnitude of wall effect is, however, smaller than that encountered in the case of cylindrical walls of an equivalent aspect ratio ($R/R_c = R/L$). Based on limited results obtained with one fall tube, Miyamura *et al.* (1981) showed that the wall effect is only a function of the aspect ratio in the low Reynolds number region. These investigators also developed empirical expressions for predicting wall effects on sphere motion settling in square and triangular containers. While both studies are related to the low Reynolds number conditions, Chow *et al.* (1989) reported limited amount of data on the drag coefficient of spheres in square channels ($R/L \approx 0.9$) at high Reynolds numbers region and found that the wall effects diminish with increasing Reynolds numbers. More recently, Balaramakrishna and Chhabra (1992) presented extensive experimental results on the free settling velocity of spheres in presence of square boundaries over a wide range of conditions. Similarly, particle motion in rectangular boundaries has received very little attention.

2.2 Non-Newtonian Media

In contrast, the contemporary literature on the free settling motion of non-spherical particles in non-Newtonian media is indeed very limited; most of it has been summarized by Chhabra (1993). One configuration which has received considerable attention is the cross flow of the viscoelastic fluids over infinitely long cylinders but rarely expressions for drag have been reported. The streamline pattern has been the main inquiry (Chhabra, 1993). Extensive literature relating to the behavior of spheres has been critically reviewed by Chhabra (1993) while the scant literature on non-spherical objects is tersely reviewed here. Brookes and Whitmore (1968, 1969) measured the drag force on cylinders, discs, ellipsoids, and prisms in Bingham plastic fluids. Some additional results for discs have also been presented by Pazwash and Robertson (1971,1975). However, owing to the unrealistic values of the yield stress used by these investigators, the reliability of their correlation is uncertain. The free settling motion of slender bodies (thin rods and wires) in power law media has been studied both theoretically as well as experimentally by

Chiba *et al.* (1986); Manero *et al.* (1987) and more recently by Unnikrishnan and Chhabra (1990). This configuration has also received some impetus from the potential of falling needle or cylinder viscometry. Apart from these investigations, limited data on the parallel motion of cylinders, cones and other irregular shaped particles in power law media have respectively been reported by Unnikrishnan and Chhabra (1990), Sharma and Chhabra (1991), Subrahmanyam and Chhabra (1990) and Venu Madhav and Chhabra (1994). Similarly, limited data on marble chips and discs are also available in the literature (Peden and Luo, 1987; Reynolds and Jones, 1989; Chhabra *et al.*, 1996, 2001). Finally it is also worthwhile to mention here that excepting the limited results on wall effects on cylinders and cones settling in power law fluids (Unnikrishnan and Chhabra, 1990; Sharma and Chhabra, 1991), no information is available on wall effects in these systems using different cross-sections of the settling vessels. This work concentrates on the effect of rectangular boundaries on the drag and settling characteristics on cylindrical particles in Newtonian fluids and shear thinning aqueous polymer solutions.

Chapter 3

Experimental materials, procedure and data analysis

In this chapter, a brief discussion of the experimental materials and method and of the data analysis and treatment procedures is presented. In particular, consideration is given to the range of different test liquids and their rheological properties, various cylindrical particles and the settling vessels for the experiments. The issue of experimental uncertainty is also addressed herein.

3.1 Test Liquids

In order to cover a wide range of particle Reynolds number and kinematical conditions, several Newtonian and non-Newtonian fluids were used as test liquids. Glucose solutions of four different concentrations have been used as Newtonian liquids in this work. The aqueous solutions of high molecular weight grade carboxymethyl cellulose, (marketed by Robert Johnson, Bombay, India) have been used as viscous non-Newtonian fluids.

All solutions were prepared using tap water as the solvent. No attempt was made to control the temperature and hence experiments were performed at room temperature. To ensure homogeneity, the solutions were mixed continuously over a period of 2-3 hours. To avoid gel formation, the solute was added in small amounts over the entire period of mixing (for the preparation CMC solutions only) in small batches. To avoid degradation by bacterial attack, 1-1.5% formaldehyde was added to the solution. The density of each test liquid was measured using a 50ml constant volume density bottle. The viscosity of Newtonian fluids was measured by the falling ball method. Four cylindrical fall tubes of different diameters were used for the viscosity measurement and a correction factor for the wall effects was made. The Haake Rotoviscometer (RV-20) was used to measure the shear stress-shear rate behavior of non-Newtonian solutions after completing the

experimental runs. (These measurements were carried out in the Department of Chemical Engineering, IIT Delhi). From the plot of shear stress versus shear rate shown in Figure (3.1), the two power-law constants, n and k (Eq. 3.1) were determined. The physical and rheological properties of all test liquids used in this work are summarized in Table 3.1. The power-law model is written as:

$$\tau = k\left(\dot{\gamma}\right)^n \tag{3.1}$$

Table 3.1 Properties of test fluids

Fluid	Temp. (K)	Density kg/m^3)	n	k(Pa.s^n)
Glucose solution (87%)	305.0	1370.00	1.0	2.6560
Glucose solution (86%)	303.5	1364.16	1.0	2.0103
Glucose solution (82%)	299.5	1328.45	1.0	0.6106
Glucose solution (80%)	301.0	1322.86	1.0	0.5132
CMC solution (3.0%)	296.5	1016.80	0.5255	21.934
CMC solution (2.5%)	296.5	1013.79	0.5475	15.068
CMC solution (2.0%)	297.0	1010.98	0.5382	8.8340
CMC solution (1.75%)	296.5	1009.98	0.5799	5.3649

3.2 Test Particles

In order to cover wide ranges of conditions, cylinders made of different materials were used in this work. The total number of cylindrical test particles used is 44, of which 9 are Teflon cylinders, 10 are glass cylinders and 25 are aluminium cylinders. The length-to diameter ratio ranges from 0.25 to 48.3. The geometrical dimensions of these test particles were measured using a micrometer (least count = 0.01mm) and a vernier caliper (least count = 0.02mm). The density of each particle was estimated by measuring the weight and the volume of particles. The dimensions and physical properties of the test particles are summarized in Appendix-A.

3.3 Fall Vessels

To study the effects of the confining walls on the settling behavior of cylindrical particles falling freely under the influence of gravity, five rectangular fall vessels made of clear Perspex were used. The important dimensions of these fall vessels are listed in Table 3.2. The rectangular fall vessel with its three major dimensions is shown in Figure (3.2). As it is seen that the width of these channels varies from 12mm to 100mm, it was not possible to drop all particles in all the fall vessels. Each fall vessel was sufficient long to accommodate 3 to 4 test sections of 50mm length. This distance is believed to sufficient for particles to achieve their terminal velocity as well for the end effects to be negligible.

Table 3.2 Dimensions of fall vessels

Sl. no.	Breadth (B) (mm)	Width (W) (mm)	Height (H) (mm)
1	363	100	600
2	375	75	600
3	210	41	600
4	274	25	600
5	270	12	600

3.4 Experimental Procedure

Test liquids were loaded into the fall vessels and the test particles were soaked in the test liquid at least 24 hours prior to the commencement of the settling tests, thereby allowing the air bubbles to escape and the thermal equilibrium to be reached. During this period the open ends of the fall vessels were covered with Perspex lids to minimize the

evaporation losses. Each vessel was ensured to be vertical within $\pm 0.5^0$ by keeping it on a plane surface.

Test particles (without any air bubbles being attached to them) were introduced into the fall vessels beneath the liquid surface with their axis parallel as well as perpendicular to that of the fall vessels and as close to its center as possible. The cylinders falling with these two orientations are shown in Figure (3.3). Only those results were accepted for which concordant fall times were obtained over two test sections. The terminal velocity of a particle was measured by timing its fall over two test sections using a stop watch reading upto 0.01 s. Each velocity value represents an average of three repeat measurements for minimizing the experimental uncertainty. In addition to the quantitative time measurement, the orientation or a change in it during settling was visually recorded. Broadly speaking, in most cases, the particles retained their initial orientation during settling.

3.5 Data Analysis

(i) Wall Effects

The confining walls or finite boundaries are known to exert an extra retardation force on freely settling particles in a viscous medium. It is necessary to introduce a wall correction factor, f, to quantify the hindrance caused by the confining walls on the terminal velocity of a particle. There are several ways of quantifying the extent of wall effects. One of the simplest definitions of the wall factor is the ratio of the terminal velocity of a particle in a bounded medium (V) to that in an unbounded medium (V_∞), i.e.,

$$f = \frac{V}{V_\infty} \tag{3.2}$$

where, V is calculated from the knowledge of fall times, and V_∞ is evaluated by extrapolating the V versus 1/h (h being the half width of rectangular channels) plots to 1/h = 0, that is $h \rightarrow \infty$. This procedure has been extensively used to correct the terminal velocity data for wall effects on spherical and non-spherical particles in both Newtonian

and non-Newtonian fluids (Uhlherr *et al.*, 1976; Unnikrishnan and Chhabra, 1991; Balaramakrishnan and Chhabra, 1992; Venumadhav and Chhabra, 1995).

To quantify the extent of wall effects in rectangular channels, the concept of hydraulic diameter has been introduced, which is defined as four times the ratio of flow area to the wetted perimeter. For cylinders in rectangular channels, the hydraulic diameter is given by:

$$D_h = \frac{4\left(2Bh - \pi d^2/4\right)}{2\left(B+2h\right)+\pi d} \tag{3.3a}$$

for vertical orientation and

$$D_h = \frac{4\left(2Bh - dl\right)}{2\left(B+2h\right)+\pi d} \tag{3.3b}$$

for horizontal orientation.

The dimensional considerations suggest the wall factor to be a function of aspect ratio of the vessel, particle-to-vessel size ratio, shape of particle and the representative Reynolds number of flow for Newtonian fluids. Additional dependence on power-law index may be expected for non-Newtonian fluids. The new experimental results will be used to establish this functional relationship between the wall factor and the other pertinent parameters.

(ii) Drag Force

At steady state condition, the drag force on a particle is balanced by its buoyant weight :

$$F_D = g.\Delta\rho \frac{\pi\, d_s^{\,3}}{6} \tag{3.4}$$

The drag force is expressed in terms of a drag coefficient as:

$$F_D = \frac{1}{2} C_d \rho_f V_\infty^{\,2} \frac{\pi d_s^{\,2}}{4} \tag{3.5}$$

Hence combining equations 3.4 and 3.5, the expression for drag coefficient is given by :

$$C_d = \frac{4}{3}\frac{g d_s}{V_\infty^{\,2}}\left(\frac{\rho_p - \rho_f}{\rho_f}\right) \tag{3.6}$$

where d_s is the equal volume sphere diameter of a cylinder, and it is given by :

$$d_s = \left(\frac{3}{2}d^2 l\right)^{1/3} \tag{3.7}$$

The dimensional analysis suggests the following definition for the Reynolds number :

$$\mathrm{Re} = \frac{d_s{}^n V_\infty{}^{2-n} \rho_f}{k} \tag{3.8}$$

where for Newtonian fluids, n = 1 and the formula reduces to,

$$\mathrm{Re} = \frac{d_s V_\infty \rho_f}{k} \tag{3.9}$$

The drag coefficient is expected to be a function of the particle Reynolds number, aspect ratio and shape of the particles. In the first instance, it is believed that the equal volume sphere diameter is sufficient to account for the particle shape. But Heiss and Coull (1952) experimented with cylinders, rectangular parallelepipeds and spheroids in Newtonian fluids, and developed two correlations for the two different orientations of the particle. The equation

$$\log_{10}(K_\infty) = \left[-0.25\sqrt{\psi\left(\frac{d_s}{d_n}\right)}\left(\frac{d_s}{d_n} - 1\right) + \log_{10}\left(\frac{d_s}{d_n}\sqrt{\psi}\right)\right] \tag{3.10}$$

is for orientations where the circularity of the projected area varies as the shape changes, and

$$\log_{10}(K_\infty) = \left[\frac{-0.27}{\sqrt{\psi\left(\frac{d_s}{d_n}\right)}^{0.345}}\left(\frac{d_s}{d_n} - 1\right) + \log_{10}\left(\frac{d_s}{d_n}\sqrt{\psi}\right)\right] \tag{3.11}$$

is for orientations where circularity is constant and does not vary as the shape of the particle changes.

In these expressions the parameter 'K_∞' is the shape correction factor, and is defined by the ratio given below:

$$K_\infty = \frac{V_\infty}{V_{s\infty}} \tag{3.12}$$

For non-spherical particles K_∞ is determined by substituting experimental data in the expression provided the Reynolds number is small,

$$K_\infty = \frac{18 V_\infty \mu}{g d_s^{\,2} (\rho_p - \rho_f)} \tag{3.13}$$

So the factor K_∞ is the ratio of the settling velocity of a cylindrical particle to that of a sphere of diameter d_s, and it is a function of d_s/d_n and Ψ for Newtonian fluids.

$$K_\infty = f\left[\left(\frac{d_s}{d_n}\right), \psi\right] \tag{3.14}$$

The diameter d_n is introduced as the diameter of a circle having the same area as the projected area of the particle in the direction of flow. So for a cylinder falling in horizontal orientation:

$$d_n = \left(\frac{4dl}{\pi}\right)^{1/2} \tag{3.15}$$

and, in vertical orientation, $d_n = d$.

The other parameter Ψ is the sphericity, and is defined as the ratio of the surface area of a sphere (of the same volume) to that of the actual particle. So for cylinders,

$$\psi = \frac{d_s^{\,2}}{\left[dl + \left(\frac{d^2}{2}\right)\right]} \tag{3.16}$$

In case of non-Newtonian fluids, factor K_∞ may also show additional dependence on the power-law index 'n', i.e.,

$$K_\infty = f\left(\psi, \frac{d_s}{d_n}, n\right) \tag{3.17}$$

Likewise, the drag coefficient may also show additional dependence on the power-law index, n. For power-law fluids, the shape correction factor is obtained by using the equation (3.12), where for non-spherical particles the modified Stokes formula is used to calculate $V_{s\infty}$ which is given as:

$$V_{s\infty} = \left(\frac{g d_s^{n+1} (\rho_p - \rho_f)}{18kX} \right)^{1/n} \tag{3.18}$$

In this equation, the parameter X is a function of 'n' and its values are given in Table (3.3).

Table 3.3 X values for a range of 'n'

n	X
1.0	1.000
0.9	1.140
0.8	1.240
0.7	1.320
0.6	1.382
0.5	1.420
0.4	1.442

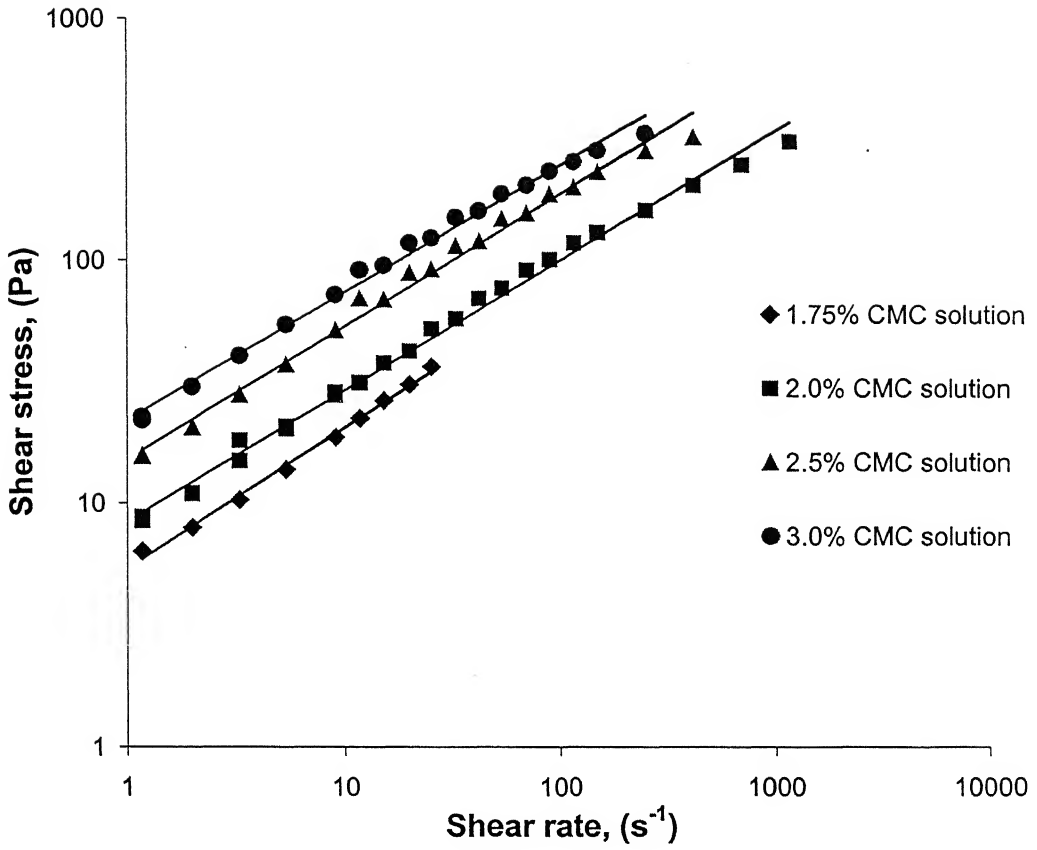

Fig. 3.1. Typical shear stress-shear rate data for four polymer solutions.

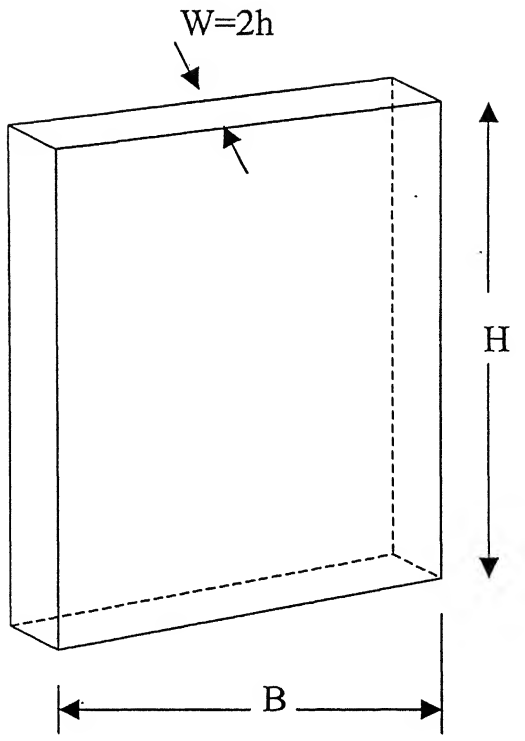

Fig. 3.2. The rectangular fall vessel with major dimensions.

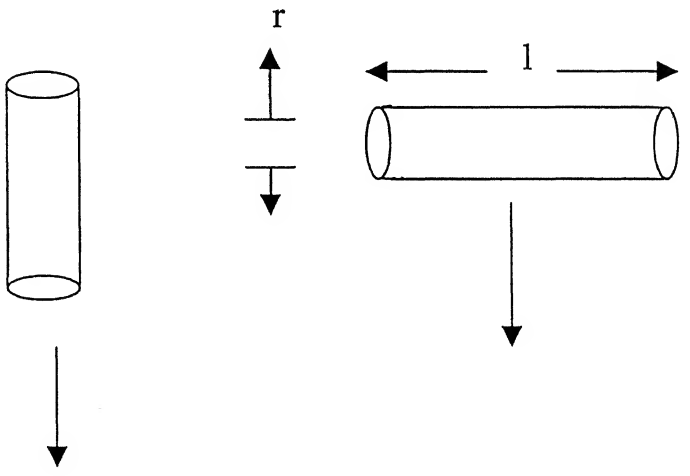

Fig. 3.3. Settling of cylindrical particle in vertical and horizontal orientations.

Chapter 4

Results and Discussion

In this chapter, the experimental results are presented and discussed. The values of drag coefficient and/or the velocity correction factors for non-spherical shape are compared with the existing frameworks for Newtonian fluids and new expressions are developed for power-law fluids. However, it is appropriate first to gauge the accuracy of the experimental results obtained in this study by analyzing the results obtained with spherical particles falling in cylindrical tubes.

4.1 Calibration Results

A few preliminary experiments were carried out with stainless steel and glass spheres to establish the reliability and overall accuracy of settling experiments. These test experiments were done with cylindrical glass tubes used as fall vessels. Figures 4.1 and 4.2 show the typical variation of the measured terminal velocity with diameter ratio for steel and glass spheres falling in 87% and 80% glucose solutions respectively. Other results for spheres also show similar behavior. The maximum value of the Reynolds number in these experiments is 0.727 and one can therefore assume the creeping flow approximation to be applicable (Clift *et al.*, 1978). One can easily extrapolate the results to d/D = 0 to get the value of V_∞, and thus calculate the value of 'f' corresponding to each fall test. Owing to the creeping flow conditions, the value of wall factor, f, is expected to depend upon the value of diameter ratio only (Clift *et al.*, 1978). The experimental values of 'f' are compared with the theoretical predictions of Faxen (1923) for $d/D < 0.1$, Haberman and Sayre (1958) for $d/D < 0.8$ and with those of Francis (1933) for $d/D < 0.97$ in Figure 4.3; the present results are seen to be in good agreement with all these predictions. The maximum discrepancy between the experimental and theoretical values is only about 8%.

The experimental values of drag coefficients are compared with the standard drag curve (Clift *et al.*, 1978) in Figure 4.4. Again, an excellent correspondence is seen to exist; the maximum error is about 5%. Based on these results it is believed that the new results obtained for cylindrical particles in this study entail an uncertainty of not more than 10%, as the same experimental techniques have been used for cylinders.

4.2 Wall effects on motion of cylinders

4.2.1 Newtonian media

Several cylinders having wide ranges of length to diameter ratio (0.125 to 48.3) were settled in different rectangular vessels with their axes parallel and perpendicular to the direction of gravity. Figures 4.5 and 4.6 show the variation of the measured terminal velocity (V) with 1/h (h being half width of rectangular vessels), for a series of cylinders settling in 86% and 80% concentrations of glucose solution with their axes parallel to the direction of gravity, and Figures 4.7 and 4.8 show the variation of the measured velocity with 1/h for the above concentrations with their axes perpendicular to the direction of gravity. Again, the dependence is seen to be linear over the range of conditions examined herein. Qualitatively similar behavior is observed when the results for the remaining cylinders and/or test solutions are plotted in this manner. This type of variation of V with d/D or 1/h has also been reported by Knudsen (1961), Kasper *et al.* (1985), Unnikrishnan and Chhabra (1991), Balaramakrishnan and Chhabra (1992), Venumadhav and Chhabra (1994) for spherical and non-spherical particles in circular as well as non-circular fall vessels.

The value of the infinite medium velocity was evaluated by extrapolating the linear relationship between V and 1/h to 1/h = 0 as seen in the Figures 4.5, 4.6, 4.7 and 4.8. This in turn allows the calculation of the wall factor for each test as a function of the hydraulic diameter of the rectangular vessels and the particle Reynolds number (based on d_s). The maximum Reynolds number is about 1.2 and so the inertial effects can be assumed to be negligible. The wall factor can thus be postulated to be independent of the Reynolds number (Chhabra, 1995).

The variation of wall factor with d/D_h for vertical and horizontal orientations is shown in figures (4.9) and (4.10) respectively. It is seen that f decreases as the d/D_h increases, though considerable scatter is present here which seems to suggest that some additional parameter is needed to account for the shape of the particle, e.g., length-to-diameter ratio and/or sphericity. A linear equation (4.1) seems to correlate the present wall factor data for vertical orientation, however, for horizontal orientation the correlation is not linear and it was necessary to use a quadratic equation (4.2).

$$f = -2.7175\left(\frac{d}{D_h}\right) + 1.0249 \tag{4.1}$$

$$f = 9.8356\left(\frac{d}{D_h}\right)^2 - 5.8113\left(\frac{d}{D_h}\right) + 1.0495 \tag{4.2}$$

Equations (4.1) and (4.2) correlates to nearly 255 data points with an average and maximum error of 28% and 72%, and 10% and 75% respectively. From these two graphs it is observed that the wall factor is a strong function of d/D_h when the cylinders fall horizontally than vertically. Hence orientation has significant effect on wall factor. Furthermore, the rather large scatter present in these figures suggests that the use of D_h is not sufficient to bring together the results for different combinations of cylinders-fall vessels. The present results for cylinders falling vertically are compared with that of Venumadhav and Chhabra (1995) and it is seen that the slope of the linear line (Equation 4.1) in the present study is much less than the value of 5.26 (Venumadhav and Chhabra, 1995) for cylinders settling in cylindrical fall vessels. This difference may account for the presence of the rectangular boundary in the present study. For a cylinder of fixed diameter, the volume equivalent diameter, d_s, varies as '$l^{1/3}$' and it is thus likely that it may be possible to show the wall factor results on the basis of d_s thereby eliminating the need to specify two geometrical parameters such as d and l or l/d. This variation is shown in Figure 4.11 and 4.12 for vertically falling and horizontally falling cylinders respectively. The wall factor variation with d_s/D_h for vertical and horizontal orientations is correlated by the following linear (4.3) and quadratic (4.4) equations respectively.

$$f = -1.3002\left(\frac{d_s}{D_h}\right) + 1.0 \tag{4.3}$$

$$f = 1.8735\left(\frac{d_s}{D_h}\right)^2 - 2.4312\left(\frac{d_s}{D_h}\right) + 1.0498 \qquad (4.4)$$

These equations fits to nearly 255 data points with an average and maximum error of 9% and 33% (Eq. 4.3), and 12% and 60% (Eq. 4.4) respectively. Though again, the wall factor decreases with increasing d_s/D_h for both orientations but this approach does not seem to offer any improvement over the previous line of analysis.

As the length-to-diameter ratio (l/d) of a cylinder is a important parameter, it is worthwhile to examine the variation of the wall factor with increasing l/d. Figures (4.13) and (4.14) show the plot of f versus l/d for vertical and horizontal orientations with limit l/d<10, and figures (4.15) and (4.16) show the respective plots for l/d>10. It is seen that for fixed diameter of cylinders, the wall factor decreases as the length of cylinders increases (l/d<10). This effect becomes more severe as the width of the rectangular fall vessels decreases. It is also observed that the slope of the wall factor versus l/d plot (for l/d<10) is higher for cylinders falling horizontally than that for the corresponding cylinders falling vertically. The wall factor becomes more pronounced for cylinders l/d>10, though it is difficult to pinpoint the critical value of l/d corresponding to this transition more accurately and hence a value of l/d = 10 is used in this work to categorize the present results. Similar type of wall factor variation over l/d is seen in Figures 4.15 and 4.16.

4.2.2 Non-Newtonian Media

It is seen that the preferred orientation for cylinders settling in rectangular vessels in non-Newtonian (CMC) solutions is with their axes parallel to the direction of gravity only irrespective of the value of l/d or the initial orientation.. Figures 4.17 and 4.18 show the variation of the terminal settling velocity with 1/h for cylinders settling in 3.0% and 1.75% carboxymethyl cellulose solutions falling vertically. The dependence is seen to be linear and similar to that observed for spheres (Chhabra *et al.*, 1977) and for cylinders (Unnikrishnan and Chhabra, 1991). The same procedure (as followed in case of Newtonian fluids) is followed to calculate the V_∞. The Reynolds number is calculated using the formula (3.8) and the maximum value of Reynolds number is found to be 0.55.

By analogy with the results for wall effects on sphere motion, the wall factor is likely to be independent of Reynolds number in the creeping flow regime. A detailed statistical analysis of data does not show any dependence of the wall factor on the power law index (n). This may be due to the rather narrow range of 'n' (0.5255 to 0.5799) covered herein. This observation is also consistent with the corresponding findings of Chhabra *et al.*, (1977) for sphere motion, and Unnikrishnan and Chhabra, (1991) for cylinder motion.

In Figure 4.19 the wall factor is plotted against d/D_h for four different concentrations of CMC solutions. The similar type behavior (as in Newtonian fluids) is also observed here. The wall factor decreases with increasing d/D_h. This relationship is well correlated by linear regression approach by the following expression:

$$f = -2.5944(d/D_h) + 1.0 \qquad (4.5)$$

The equation (4.5) represents 410 data points with average and maximum error of 20% and 46% respectively. This slope is less than the value of 3.85 (Venumadhav and Chhabra, 1995) for cylinders settling in cylindrical fall vessels. This difference may account for the presence of the rectangular boundary in the present study. The wall factor is also plotted against d_s/D_h in Figure 4.20, which also shows a linear dependence of wall factor with d_s/D_h. This is correlated by the expression:

$$f = -0.9089(d_s/D_h) + 1.0 \qquad (4.6)$$

This equation correlates with 410 data points with an average and maximum error of 17% and 44% respectively.

As length-to-diameter ratio is an important parameter affects the wall factor, it is necessary to show the variation of f with l/d of cylinders. Figures 4.21 and 4.22 show this variation for cylinders having $l/d<10$ and $l/d>10$ respectively in 2.0% CMC solution. The value of wall factor decreases with increasing l/d (for a fixed 'd') linearly and the slope increases as the width of the fall vessels decreases. This behavior is also seen in case of Newtonian fluids. Similar plots are obtained for other concentrations.

It is important to make observations with the Newtonian and non-Newtonian fluids. By comparing the plots and statistically analyzing the wall factor data herein, it is seen that the wall effects are less severe in non-Newtonian (shear-thinning) fluids than in Newtonian fluids.

4.3 Drag coefficient results

4.3.1 Newtonian Media

From a knowledge of V_∞ and the other physical properties of test fluids and test particles, the value of C_d as a function of Reynolds number and l/d was calculated for each individual fall test of particle. The value of Re ranges from 0.001 to 1.2, hence creeping flow was assumed throughout the calculations. The values of C_d are plotted against Re on a logarithmic coordinates in Figure (4.23). As 'd_s' is used for the calculation of Re and C_d, the particle orientation doesn't have any effect on C_d. In figure (4.23), the present drag results are compared with equation (4.7) (Venumadhav and Chhabra, 1994) which is given as;

$$C_d = \frac{24}{\mathrm{Re}}\left(1 + 0.604\,\mathrm{Re}^{0.529}\right) \qquad \text{for } 0.1 < \mathrm{Re} < 423 \qquad (4.7)$$

The resulting overall mean and maximum deviations between the predictions of equation (4.7) and the present data are 23.7% and 76.5% 128 data points. This deviation may be due to the very low ranges of Reynolds numbers ($0.01 < \mathrm{Re} < 1.2$) in this work. Hence it can be concluded that the equation (4.7) is not satisfactory for such low values of Reynolds numbers and/or for both orientations (vertical and horizontal) of cylinder. This comparison suggests that some additional parameter is needed to account for the orientation of the cylinder, e.g., projected area (A_p) of cylinder.

The effect of orientation on the settling velocity can also be quantified by the settling factor K_∞. A quantitative comparison of data between the experimental and theoretical results for K_∞ is shown in Tables (4.1) and (4.2) for 87% and 86% glucose solution for vertical orientation and in Tables (4.3) and (4.4) for the above two concentrations for horizontal orientation. The experimental K_∞ values were calculated using equation (3.13) whereas the values due to Heiss and Coull (1952) were obtained from equations (3.10) and (3.11) for horizontal and vertical orientations respectively. Some results show appreciable deviations from the predictions of equations (3.10) and (3.11). This may be due to the unstable settling of some cylinders as indicated in these tables.. Again the l/d ratios of cylinders used in this work (4.0 to 48.3) are beyond the range covered by the equations (3.10) and (3.11) (0.125 to 4), hence this range of l/d

(>4.0) may also account for the deviation in K_∞ values. However, we can conclude that the free settling velocity and hence the drag coefficient is affected principally by the orientation, the sphericity and the d_s/d_n of the particle.

4.3.2 Non-Newtonian Media

For power law shear-thinning liquid flow around a cylinder, one can expect the dependence of drag coefficient on the particle Reynolds number, and with the power law index 'n'. Hence the functional relationship is given by;

$$C_d = f(\mathrm{Re}, n) \tag{4.8}$$

The Reynolds number is calculated by using the formula;

$$\mathrm{Re} = \frac{d_s{}^n V_\infty{}^{2-n} \rho}{k} \tag{4.9}$$

The maximum Reynolds number is found to be 0.55 and hence the creeping flow regime is well assumed. For each particle falling vertically, the value of C_d was calculated as a function of Re. The drag coefficient is plotted against Reynolds number on a logarithmic plot and compared with the correlation, equation (4.7) (Venumadhav and Chhabra, 1994) in Figure (4.24). A fair agreement is seen to exist with average and maximum deviations of 8.0% and 21.4% for 95 data points despite very low Reynolds number range (Re<0.55) and n values (0.5255 to 0.5799) in the present study (for equation (4.7), the range of Reynolds number is 0.1 to 423 and 'n' is 1.0). The behavior is similar to that of Newtonian fluids.

A comparison between the experimental and theoretical K_∞ values is shown in Tables (4.5), (4.6), (4.7) and (4.8) for 1.75 %, 2.0%, 2.5% and 3.0% CMC solutions respectively. It is seen that for cylinders having l/d > 10, the agreement seems good except for certain cylinders with unstable settling conditions. This deviation of the present results from equation (3.11) may be due to the higher l/d ratios (>4.0) used in the

of the flow behavior index 'n'.

Table 4.1. Comparison of experimental K_∞ values with those obtained from Heiss-Coull correlation (equation 3.11) for cylinders falling vertically in 87.0% glucose solution.

d_s/d_n	ψ	l/d	K_∞(Eq. 3.11)	K_∞(Experimental)
3.3413	0.440	24.87	0.521303	0.360129
3.0810	0.474	19.50	0.592983	0.424816
2.4661	0.579	10.00	0.780427	0.517628
1.9574	0.696	5.000	0.927294	0.504237*
1.9242	0.705	4.750	0.935890	0.531315*
4.1685	0.356	48.30	0.330760	0.210847
3.8000	0.389	36.58	0.407385	0.247190
2.8600	0.508	15.60	0.659108	0.421500
2.6170	0.550	11.95	0.733769	0.471389
2.0340	0.677	5.600	0.907940	0.702800*
3.9900	0.371	42.40	0.365926	0.360600
3.1795	0.461	21.40	0.565849	0.416580
2.4560	0.581	9.800	0.783503	0.662870
2.2910	0.616	8.000	0.833999	0.735580
2.0822	0.665	6.000	0.894798	0.747220
1.8189	0.733	4.000	0.959996	0.841900
2.4385	0.585	9.670	0.789465	0.693240
2.2894	0.616	8.000	0.834056	0.716900
2.0606	0.670	5.830	0.900359	0.754180
1.8169	0.733	4.000	0.959898	0.843180
2.4560	0.581	9.850	0.783611	0.683510
2.2921	0.616	8.000	0.833960	0.689940
2.1034	0.660	6.200	0.889112	0.717780
2.7513	0.526	13.80	0.692162	0.622336
2.4037	0.592	9.259	0.799953	0.741690

* Unstable settling

Table 4.2. Comparison of experimental K_∞ values with those obtained from Heiss-Coull correlation (equation 3.11) for cylinders falling vertically in 86.0% glucose solution.

d_s/d_n	ψ	l/d	K_∞(Eq. 3.11)	K_∞(Experimental
3.3413	0.440	24.87	0.521303	0.376391
3.0810	0.474	19.50	0.592983	0.379330
2.4661	0.579	10 .00	0.780427	0.471364
1.9574	0.696	5.000	0.927294	0.647481*
1.9242	0.705	4.750	0.935890	0.632365*
4.1685	0.356	48.30	0.330760	0.371594
3.8000	0.389	36.58	0.407385	0.363739
2.8600	0.508	15.60	0.659108	0.574092
2.6170	0.550	11.95	0.733769	0.587437
2.0340	0.677	5.600	0.907940	0.722208*
3.9900	0.371	42.40	0.365926	0.364608
3.1795	0.461	21.40	0.565849	0.482715
2.4560	0.581	9.800	0.783503	0.690113
2.2910	0.616	8.000	0.833999	0.728169
2.0822	0.665	6.000	0.894798	0.798111
1.8189	0.733	4.000	0.959996	0.896429
2.4384	0.585	9.670	0.789465	0.694074
2.2894	0.616	8.000	0.834056	0.741083
2.0606	0.670	5.830	0.900359	0.814711
1.8169	0.733	4.000	0.959898	0.919226
2.4540	0.581	9.850	0.783611	0.688579
2.2921	0.616	8.000	0.833960	0.720137
2.1034	0.660	6.200	0.889112	0.748216
2.7513	0.526	13.80	0.692162	0.641814
2.4037	0.592	9.259	0.799953	0.739599

* Unstable settling

Table 4.3. Comparison of experimental K_∞ values with those obtained from Heiss-Coull correlation (equation 3.10) for cylinders falling horizontally in 87.0% glucose solution.

d_s/d_n	ψ	l/d	K_∞(Eq. 3.10)	K_∞(Experimental)
0.59370	0.440	24.87	0.443822	0.183094*
0.61833	0.474	19.50	0.479475	0.231332*
0.69113	0.579	10.00	0.588499	0.385000
0.77577	0.696	5.000	0.711588	0.550028
0.78245	0.705	4.750	0.721020	0.541783
0.53160	0.356	48.30	0.356658	0.173318*
0.55676	0.389	36.58	0.391031	0.208566*
0.64168	0.508	15.60	0.514517	0.376840
0.67090	0.550	11.95	0.558235	0.436181
0.76100	0.677	5.600	0.691140	0.518359
0.54323	0.371	42.40	0.372336	0.160427*
0.60871	0.461	21.40	0.465672	0.268171*
0.69257	0.581	9.800	0.590622	0.478766
0.71696	0.616	8.000	0.627061	0.530028
0.75217	0.665	6.000	0.678494	0.606084
0.80470	0.733	4.000	0.751077	0.691980
0.69500	0.585	9.670	0.594541	0.495038
0.71730	0.616	8.000	0.627293	0.538443
0.75610	0.670	5.830	0.683936	0.607460
0.80510	0.733	4.000	0.751333	0.680227
0.69284	0.581	9.850	0.590801	0.495293
0.71686	0.616	8.000	0.626993	0.553952
0.84838	0.660	6.200	0.735743	0.600217
0.65427	0.526	13.80	0.533278	0.448497
0.70000	0.592	9.259	0.601921	0.526838

* Unstable settling

Table 4.4. Comparison of experimental K_∞ values with those obtained from Heiss-Coull correlation (equation 3.10) for cylinders falling horizontally in 86.0% glucose solution.

d_s/d_n	ψ	l/d	K_∞(Eq. 3.10)	K_∞(Experimental)
0.59370	0.440	24.87	0.443822	0.153570*
0.61833	0.474	19.50	0.479475	0.180016*
0.69113	0.579	10.00	0.588499	0.195020
0.77577	0.696	5.000	0.711588	0.309575
0.78245	0.705	4.750	0.721020	0.336438
0.53160	0.356	48.30	0.356658	0.137965*
0.55676	0.389	36.58	0.391031	0.178914*
0.64168	0.508	15.60	0.514517	0.345048
0.67090	0.550	11.95	0.558235	0.391600
0.76100	0.677	5.600	0.691140	0.652000
0.54323	0.371	42.40	0.372336	0.154625*
0.60871	0.461	21.40	0.465672	0.259600*
0.69257	0.581	9.800	0.590622	0.475600
0.71696	0.616	8.000	0.627061	0.523600
0.75217	0.665	6.000	0.678494	0.608350
0.80470	0.733	4.000	0.751077	0.673700
0.69500	0.585	9.670	0.594541	0.512100
0.71730	0.616	8.000	0.627293	0.555200
0.75610	0.670	5.830	0.683936	0.685000
0.80510	0.733	4.000	0.751333	0.669000
0.69284	0.581	9.850	0.590801	0.526898
0.71686	0.616	8.000	0.626993	0.566360
0.84838	0.660	6.200	0.735743	0.664200
0.65427	0.526	13.80	0.533278	0.463200
0.70000	0.592	9.259	0.601921	0.659800

* Unstable settling

Table 4.5. Comparison of experimental K_∞ values with those obtained from Heiss-Coull correlation (equation 3.11) for cylinders falling vertically in 1.75% CMC solution.

d_s/d_n	ψ	l/d	K_∞(Eq. 3.11)	K_∞(Experimental)
3.3413	0.440	24.87	0.521303	0.575769
3.0810	0.474	19.50	0.592983	0.573508
2.4661	0.579	10.00	0.780427	0.838911
1.9574	0.696	5.000	0.927294	1.435488
1.9243	0.705	4.750	0.935890	1.400958
4.1685	0.356	48.30	0.330760	0.442797
3.8000	0.389	36.58	0.407385	0.542340
2.8600	0.508	15.60	0.659108	1.004390*
2.6170	0.550	11.95	0.733769	1.251541*
3.9900	0.371	42.40	0.365926	0.435638
3.1795	0.461	21.40	0.565849	0.715245
2.4560	0.581	9.800	0.783503	1.356713
2.2910	0.616	8.000	0.833999	1.514683
2.0822	0.665	6.000	0.894798	1.786073
1.8189	0.733	4.000	0.959996	2.146172
2.4385	0.585	9.670	0.789465	1.448575
2.2894	0.616	8.000	0.834056	1.567278
2.0606	0.670	5.830	0.900359	1.884390
1.8169	0.733	4.000	0.959898	2.188733
2.4540	0.581	9.850	0.783611	1.498582
2.2921	0.616	8.000	0.833960	1.634146
2.1034	0.660	6.200	0.889112	1.880395
2.7513	0.526	13.80	0.692162	1.332577*
2.4037	0.592	9.259	0.799953	1.679640

* Unstable settling

Table 4.6. Comparison of experimental K_∞ values with those obtained from Heiss-Coull correlation (equation 3.11) for cylinders falling vertically in 2.0% CMC solution.

d_s/d_n	ψ	l/d	K_∞(Eq. 3.11))	K_∞(Experimental)
3.3413	0.440	24.87	0.5213	0.4354
3.0810	0.474	19.50	0.5930	0.5137
2.4661	0.579	10.00	0.7804	0.8923
1.9574	0.696	5.000	0.9273	1.3406
1.9243	0.705	4.750	0.9359	1.3361
4.1685	0.356	48.30	0.3308	0.4011
3.8000	0.389	36.58	0.4074	0.4764
2.8600	0.508	15.60	0.6591	0.8995*
2.6170	0.550	11.95	0.7338	1.0486*
2.0340	0.677	5.600	0.9079	1.6965
3.9900	0.371	42.40	0.3659	0.3832
3.1795	0.461	21.40	0.5658	0.6032
2.4560	0.581	9.800	0.7835	1.2041
2.2910	0.616	8.000	0.8340	1.3940
2.0822	0.665	6.000	0.8948	1.5444
1.8189	0.733	4.000	0.9600	1.9886
2.4385	0.585	9.670	0.7895	1.3400
2.2894	0.616	8.000	0.8341	1.4672
2.0606	0.670	5.830	0.9004	1.6109
1.8169	0.733	4.000	0.9599	2.1295
2.4540	0.581	9.850	0.7836	1.3639
2.2921	0.616	8.000	0.8340	1.5394
2.1034	0.660	6.200	0.8891	1.7411
2.7513	0.526	13.80	0.6922	1.2483*
2.4037	0.592	9.259	0.8000	1.6327

* Unstable settling

Table 4.7. Comparison of experimental K_∞ values with those obtained from Heiss-Coull correlation (equation 3.11) for cylinders falling vertically in 2.5% CMC solution.

d_s/d_n	ψ	l/d	K_∞(Eq. 3.11)	K_∞(Experimental)
3.3413	0.440	24.87	0.5213	0.476144
3.0801	0.474	19.50	0.5930	0.586582
2.4661	0.579	10.00	0.7804	1.043100
1.9574	0.696	5.000	0.9273	1.475771
1.9243	0.705	4.750	0.9359	1.479427
4.1685	0.356	48.30	0.3308	0.395597
3.8000	0.389	36.58	0.4074	0.469169
2.8600	0.508	15.60	0.6591	0.847458*
2.6170	0.550	11.95	0.7338	1.057692*
3.9900	0.371	42.40	0.3659	0.399916
3.1795	0.461	21.40	0.5658	0.600000
2.4560	0.581	9.800	0.7835	1.210026
2.2910	0.616	8.000	0.8340	1.365546
2.0822	0.665	6.000	0.8948	1.652893
1.8189	0.733	4.000	0.9600	1.818182
2.4385	0.585	9.670	0.7895	1.206140
2.2894	0.616	8.000	0.8341	1.310616
2.0606	0.670	5.830	0.9004	1.587301
1.8169	0.733	4.000	0.9599	1.763224
2.4540	0.581	9.850	0.7836	1.251739
2.2921	0.616	8.000	0.8340	1.349073
2.1034	0.660	6.200	0.8891	1.505376
2.7513	0.526	13.80	0.6922	1.025641*
2.4037	0.592	9.259	0.8000	1.387283

* Unstable settling

Table 4.8. Comparison of experimental K_∞ values with those obtained from Heiss-Coull correlation (equation 3.11) for cylinders falling vertically in 3.0% CMC solution.

d_s/d_n	ψ	l/d	K_∞(Eq. 3.11)	K_∞(Experimental)
3.3413	0.440	24.87	0.521303	0.458529
3.0810	0.474	19.50	0.592983	0.541586
2.4611	0.579	10.00	0.780427	0.812008
1.9573	0.696	5.000	0.927294	1.251203
1.9243	0.705	4.750	0.935890	1.263903
4.1685	0.356	48.30	0.330760	0.298619
3.8000	0.389	36.58	0.407385	0.385742
2.8600	0.508	15.60	0.659108	0.790646*
2.6170	0.550	11.95	0.733769	0.994236*
2.0340	0.677	5.600	0.907940	1.796407
3.9900	0.371	42.40	0.365926	0.334971
3.1795	0.461	21.40	0.565849	0.518135
2.4560	0.581	9.800	0.783503	1.048544
2.2910	0.616	8.000	0.833999	1.235154
2.0822	0.665	6.000	0.894798	1.489028
1.8189	0.733	4.000	0.959996	1.813954
2.4385	0.585	9.670	0.789465	1.138614
2.2894	0.616	8.000	0.834056	1.190476
2.0606	0.670	5.830	0.900359	1.491935
1.8169	0.733	4.000	0.959898	1.627907
2.4540	0.581	9.850	0.783611	1.050633
2.2921	0.616	8.000	0.833960	1.150579

* Unstable settling

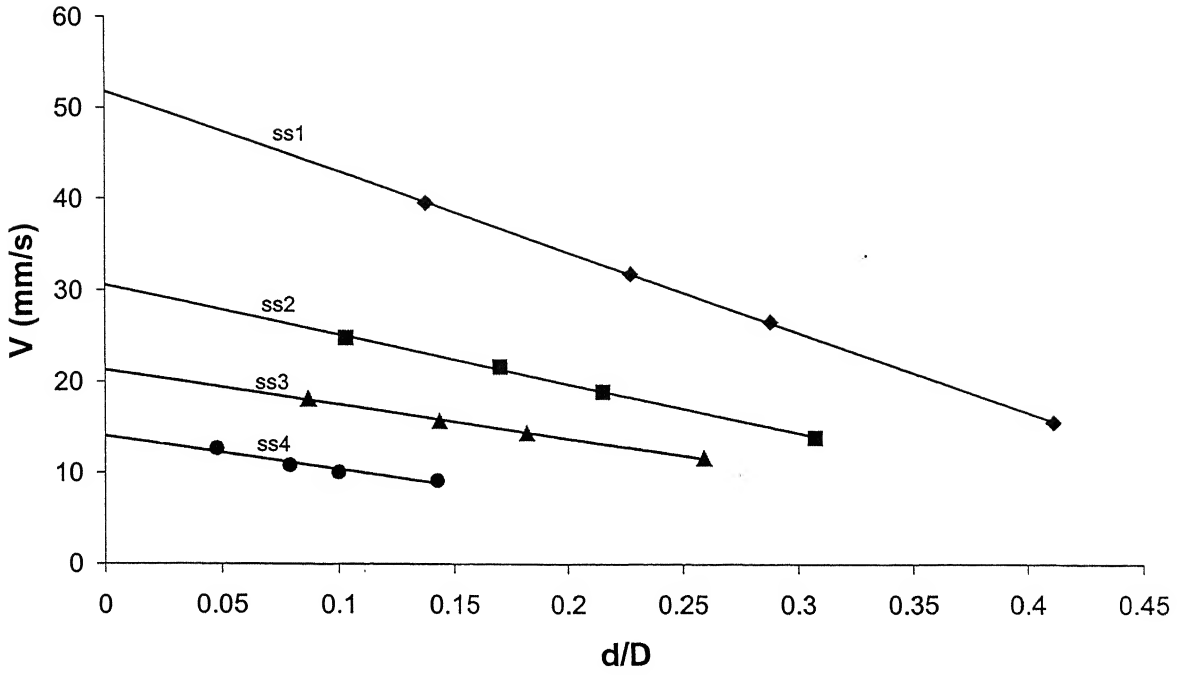

Fig. 4.1. Variation of measured velocity with diameter of fall tubes in 87% glucose solution.

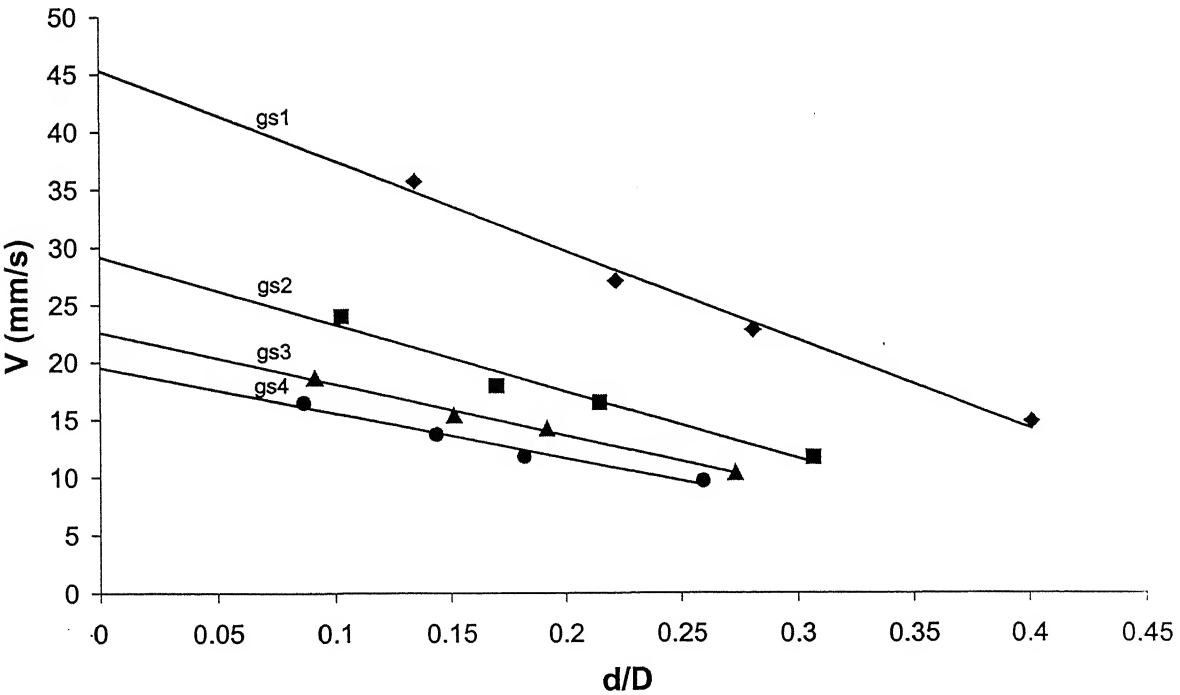

Fig. 4.2. Variation of measured velocity with diameter of fall tubes in 80% glucose solution.

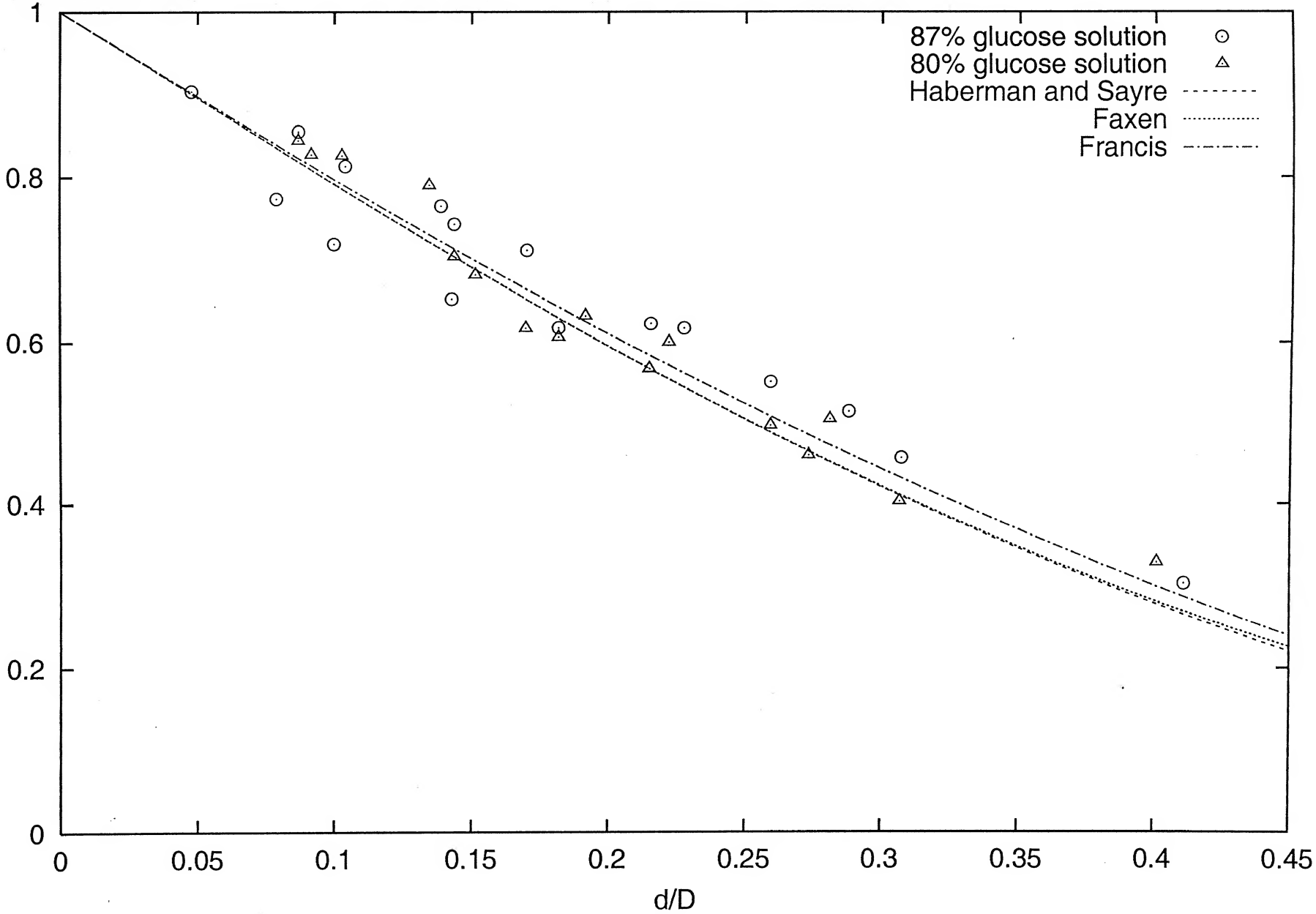

Fig. 4.3. Comparison of the present values of wall factor with the literature results for spheres.

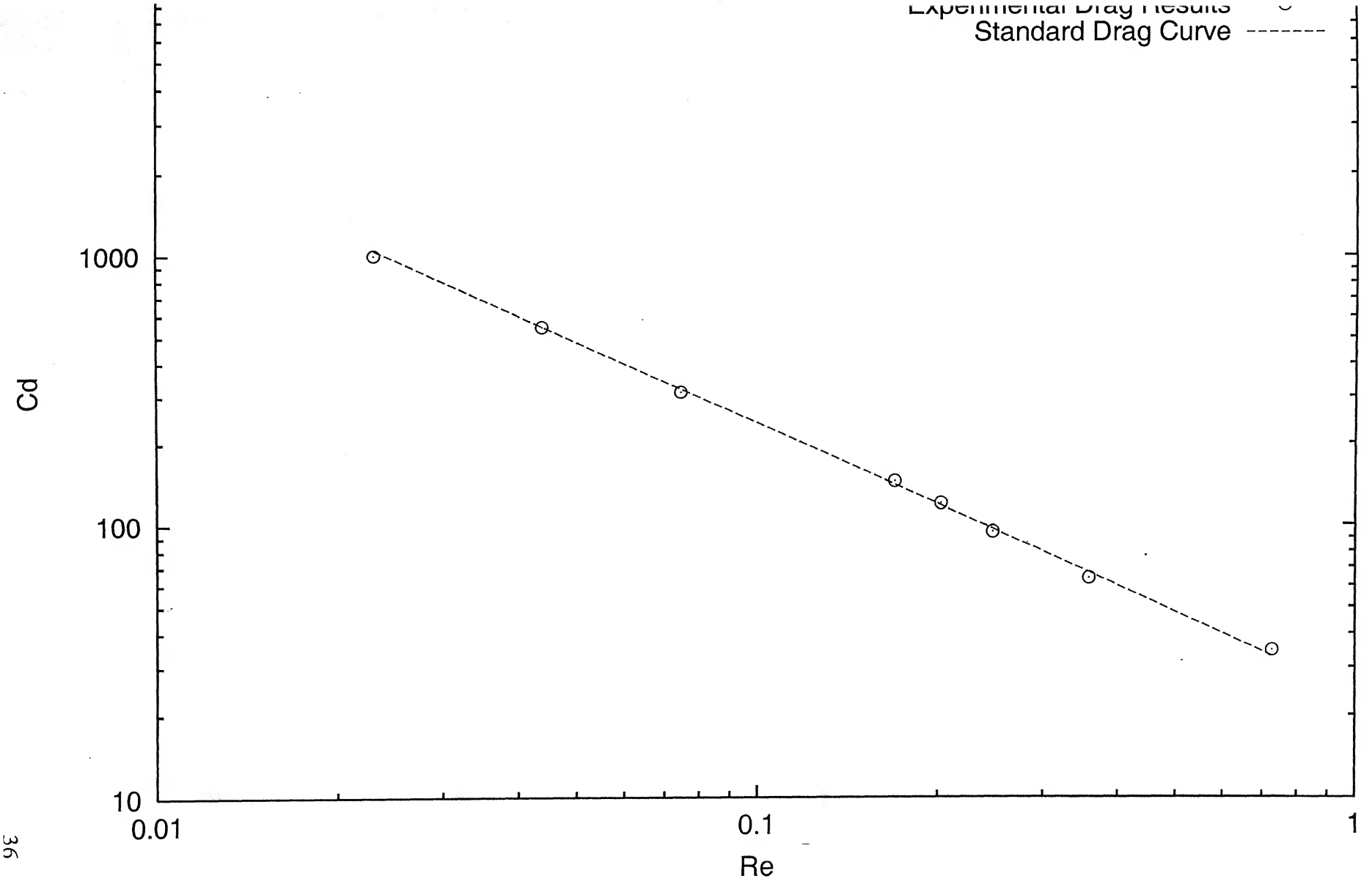

Fig. 4.4. Comparison of the present values of C_d with the literature results for spheres.

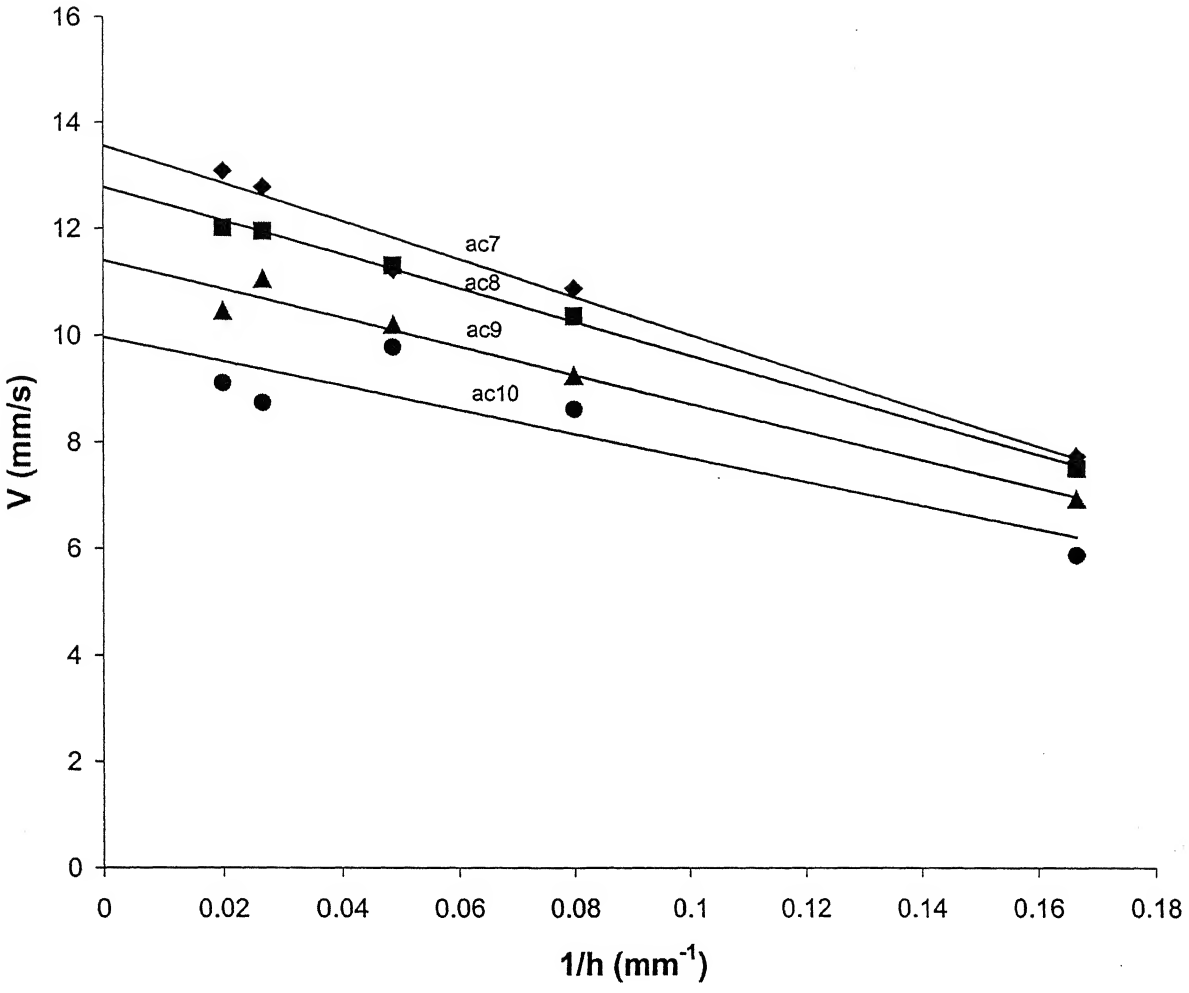

Fig. 4.5. Variation of settling velocity with width of rectangular vessels in 86% glucose solution (vertical orientation).

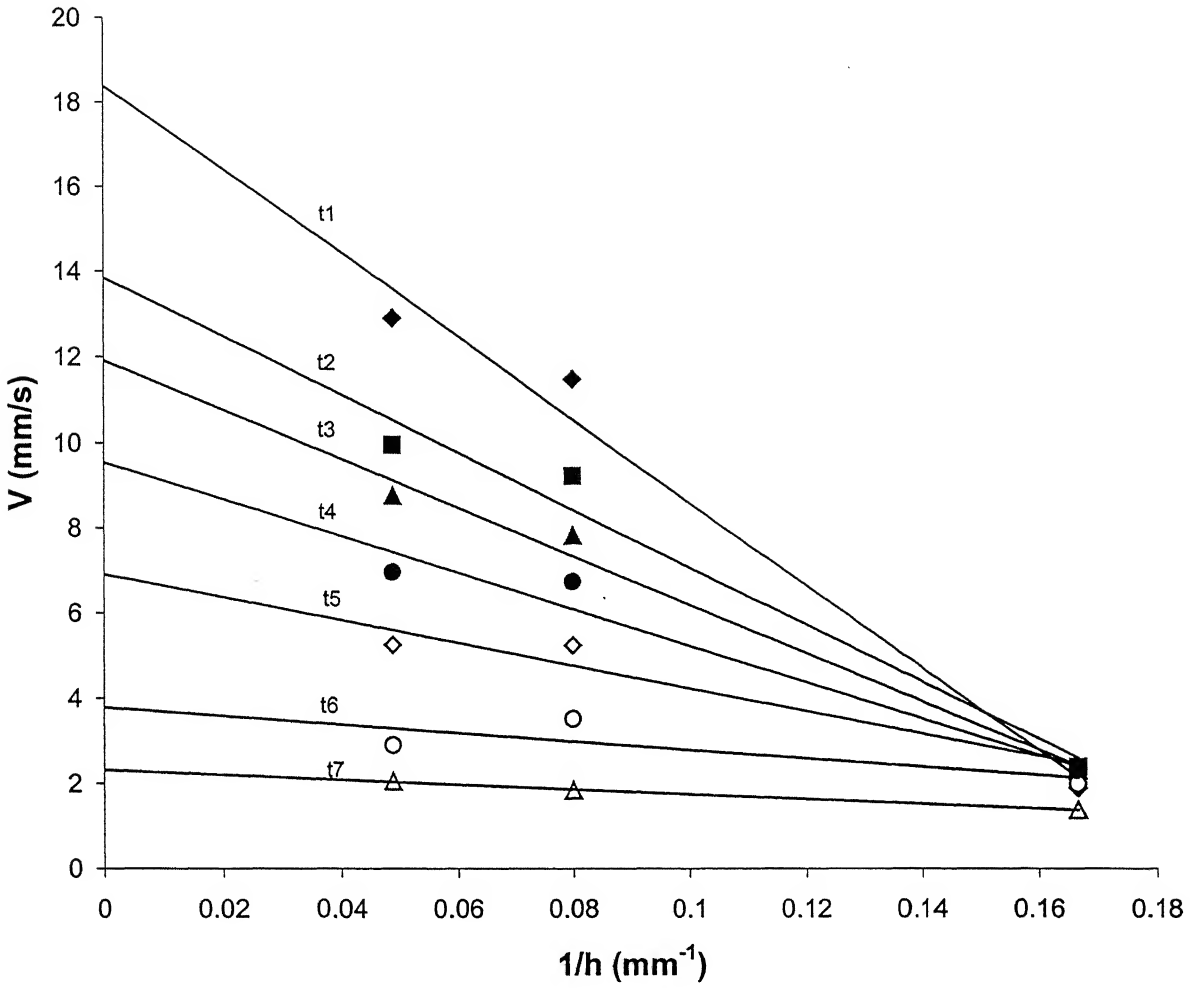

Fig. 4.6. Variation of settling velocity with width of rectangular vessels in 80% glucose solution (vertical orientation).

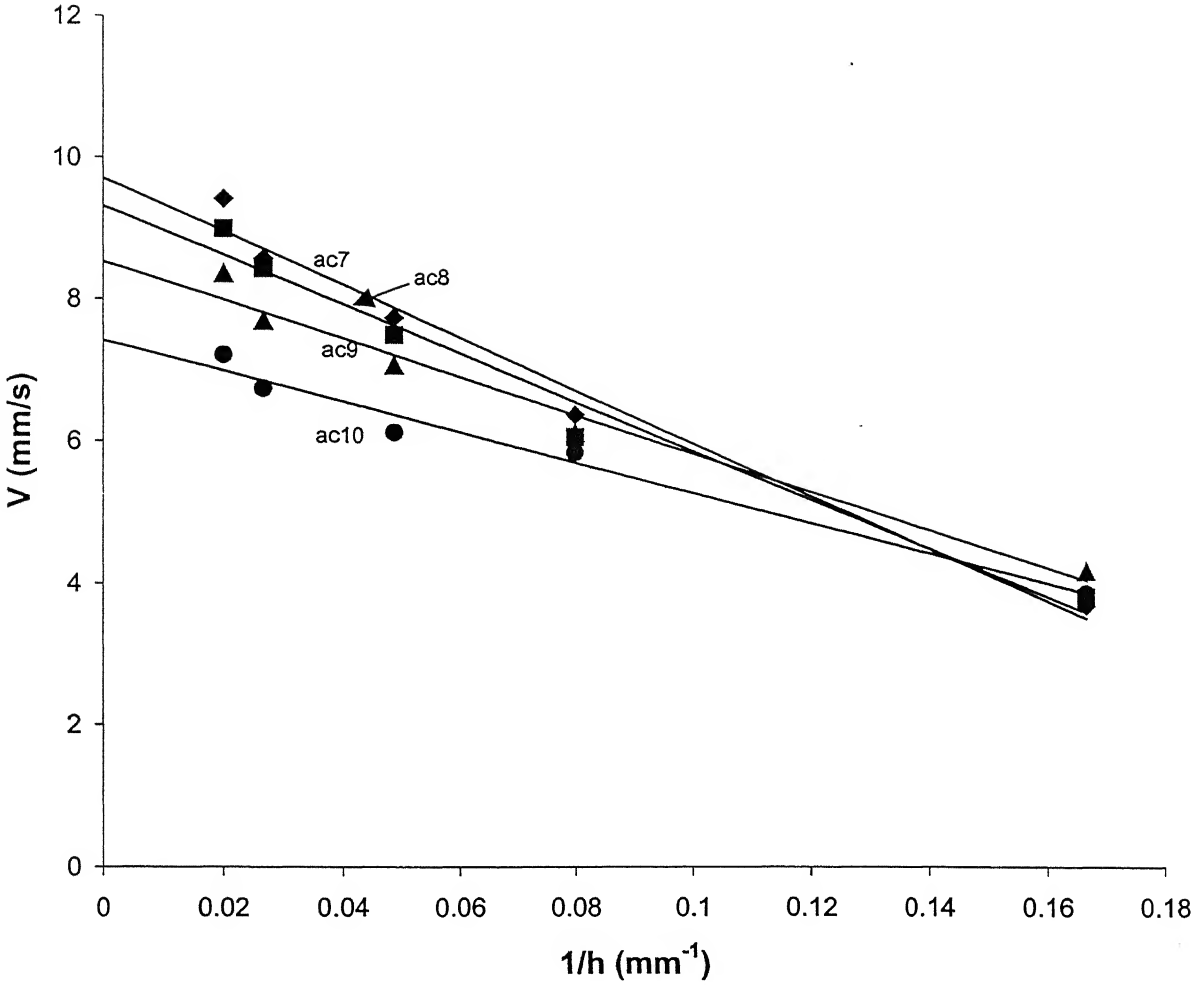

Fig. 4.7. Variation of settling velocity with width of the rectangular vessels in 86% glucose solution (horizontal orientation).

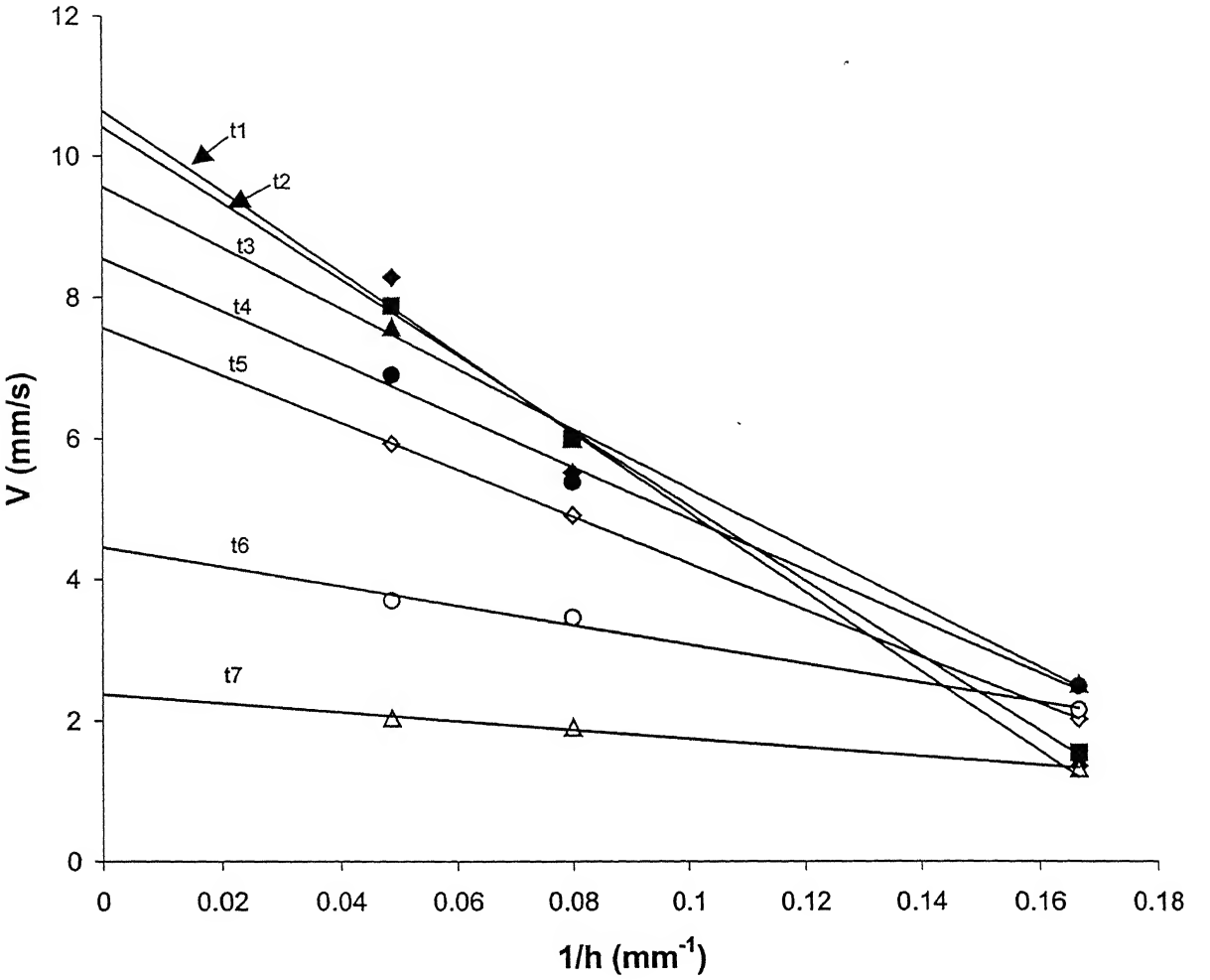

Fig. 4.8. Variation of settling velocity with width of rectangular vessels in 80% glucose solution (horizontal orientation).

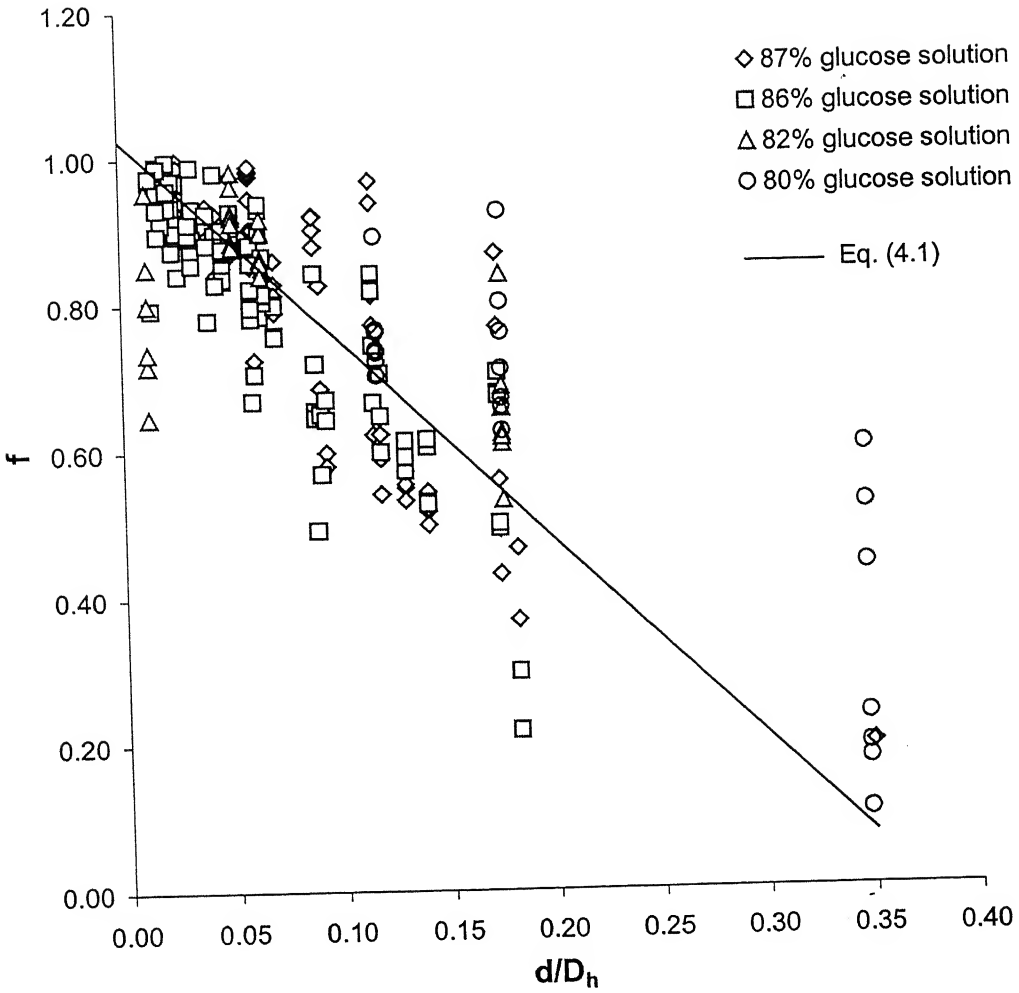

Fig. 4.9. Wall factor for cylinders falling vertically as a function of d/D_h (Newtonian media).

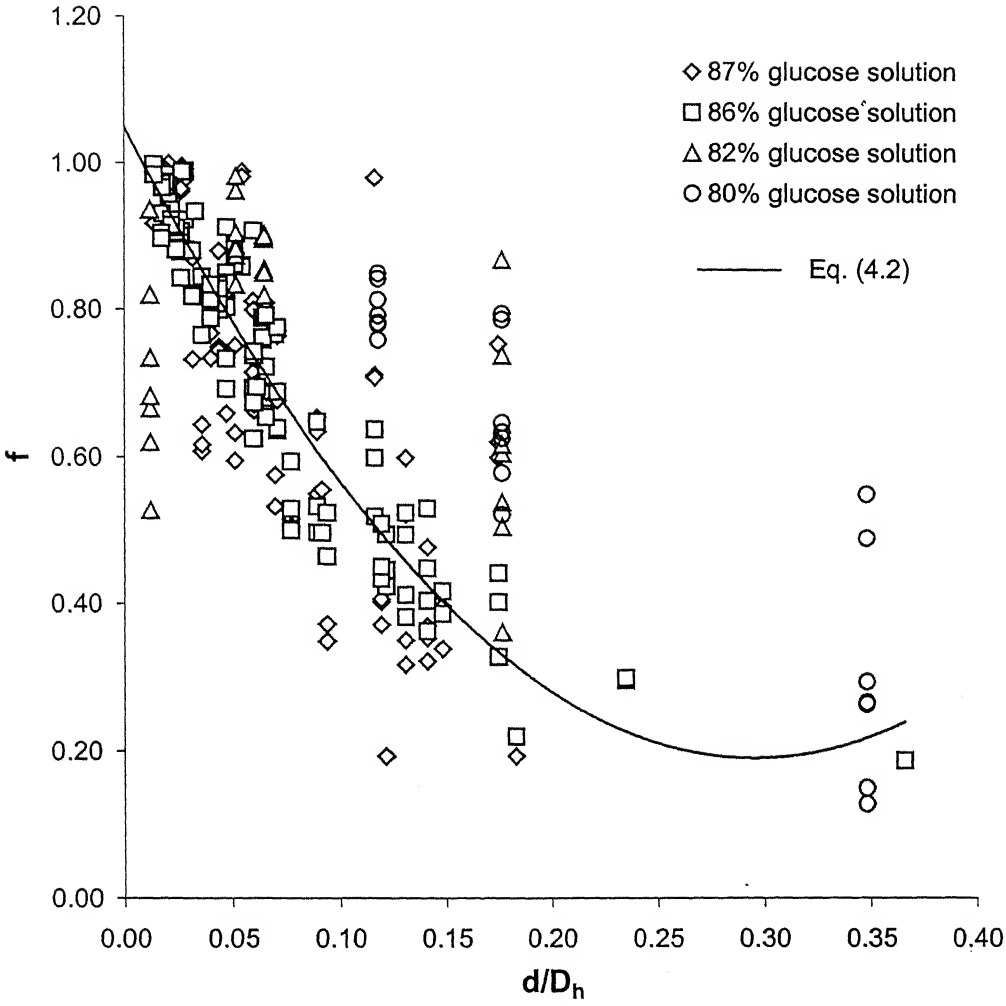

Fig. 4.10. Wall factor for cylinders falling horizontally as a function of d/D_h (Newtonian media).

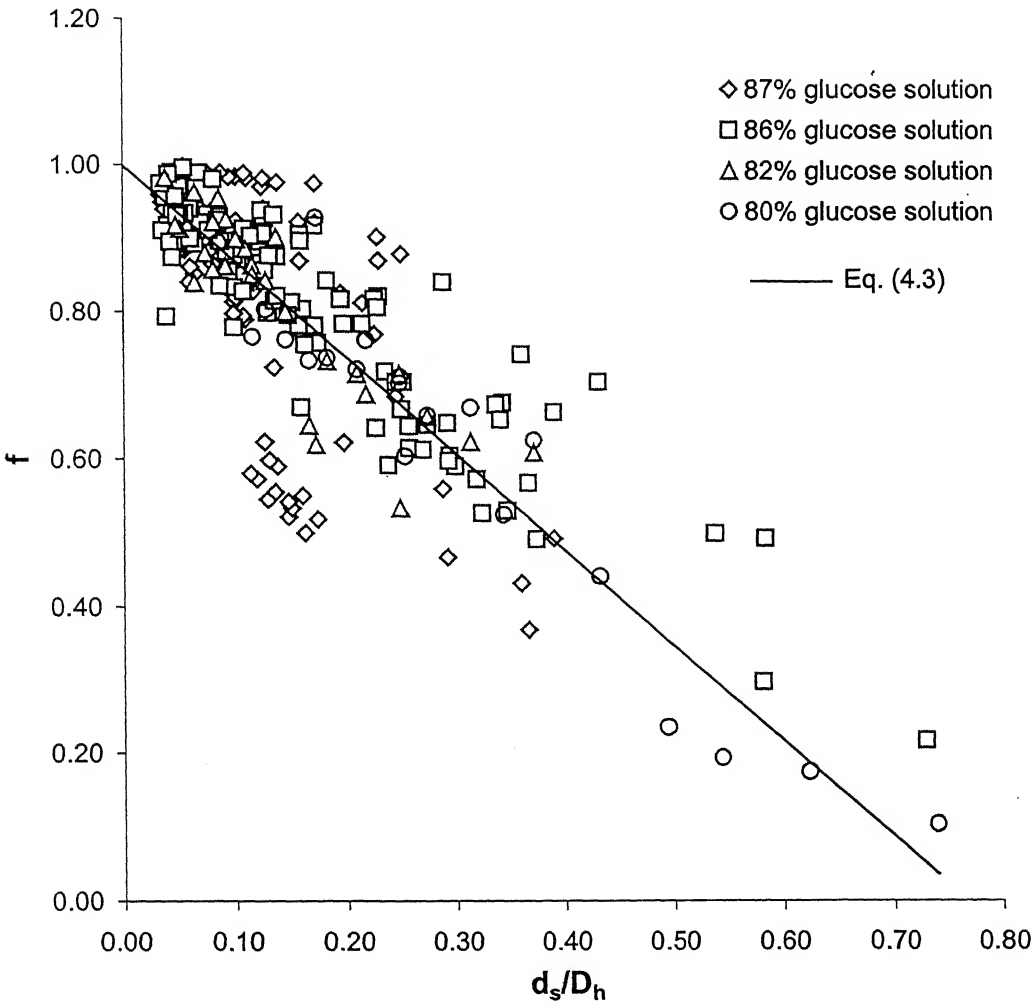

Fig. 4.11. Wall factor for cylinders falling vertically as a function of d_s/D_h (Newtonian media).

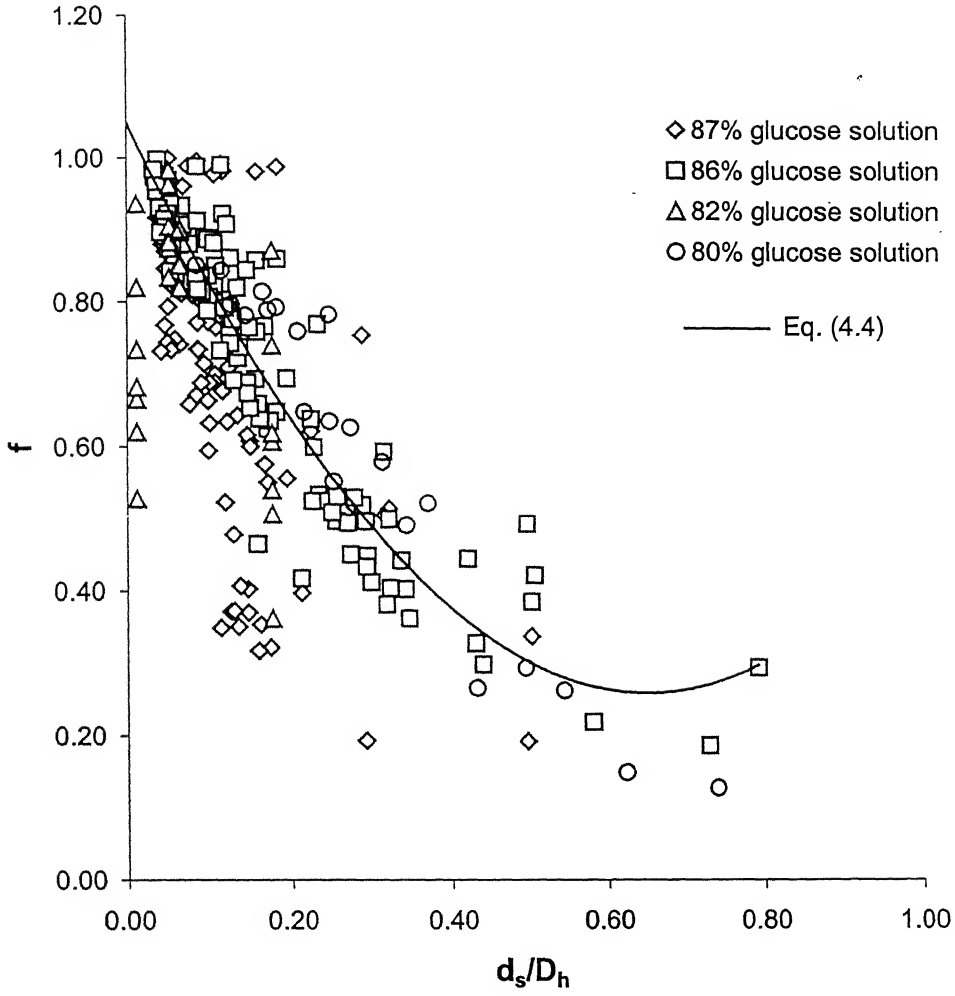

Fig. 4.12. Wall factor for cylinders falling horizontally as a function of d_s/D_h (Newtonian media).

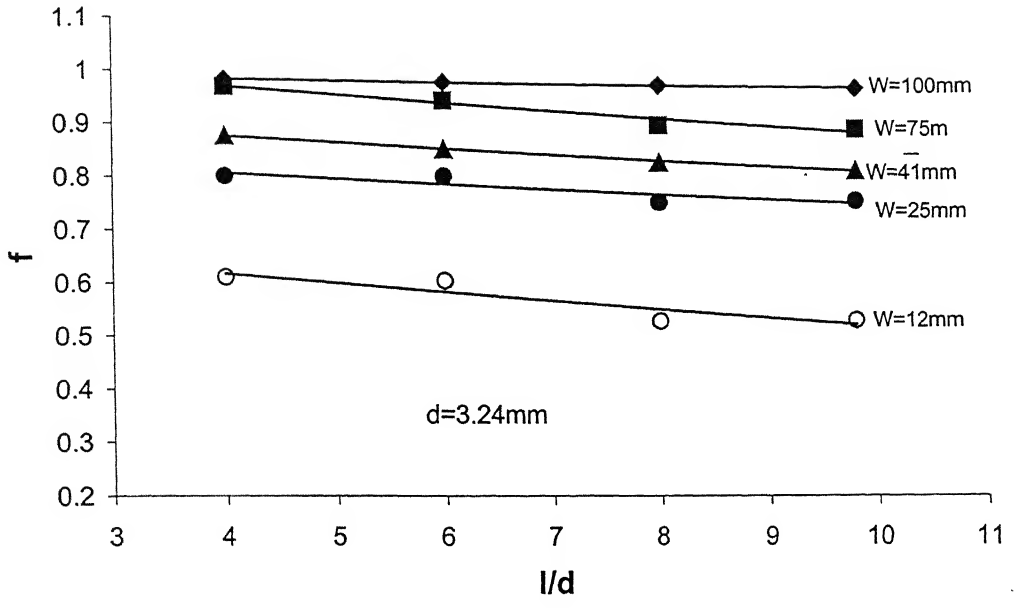

Fig. 4.13. Wall factor for short cylinders (l/d<10) falling vertically as a function of l/d.

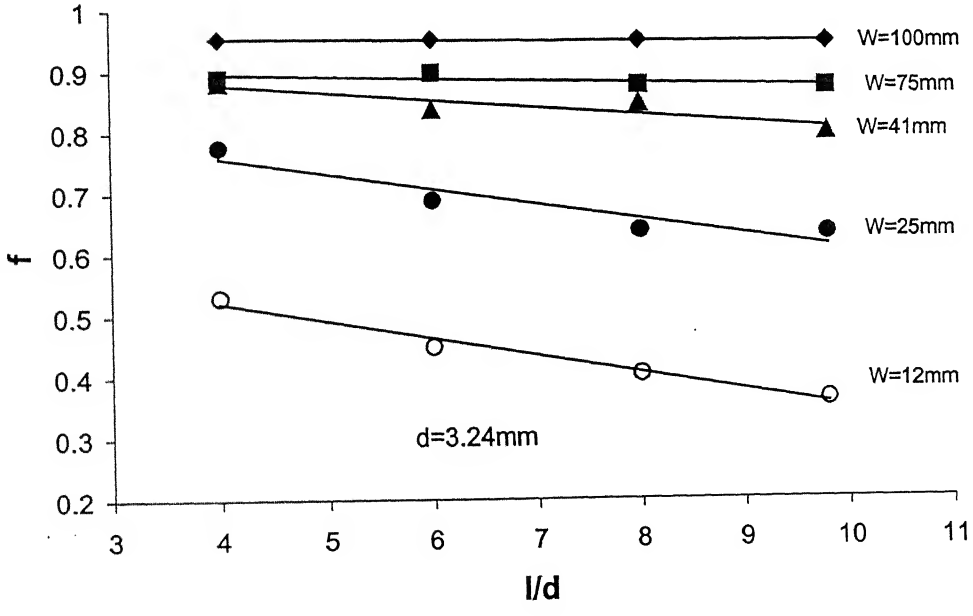

Fig. 4.14. Wall factor for short cylinders (l/d<10) falling horizontally as a function of l/d.

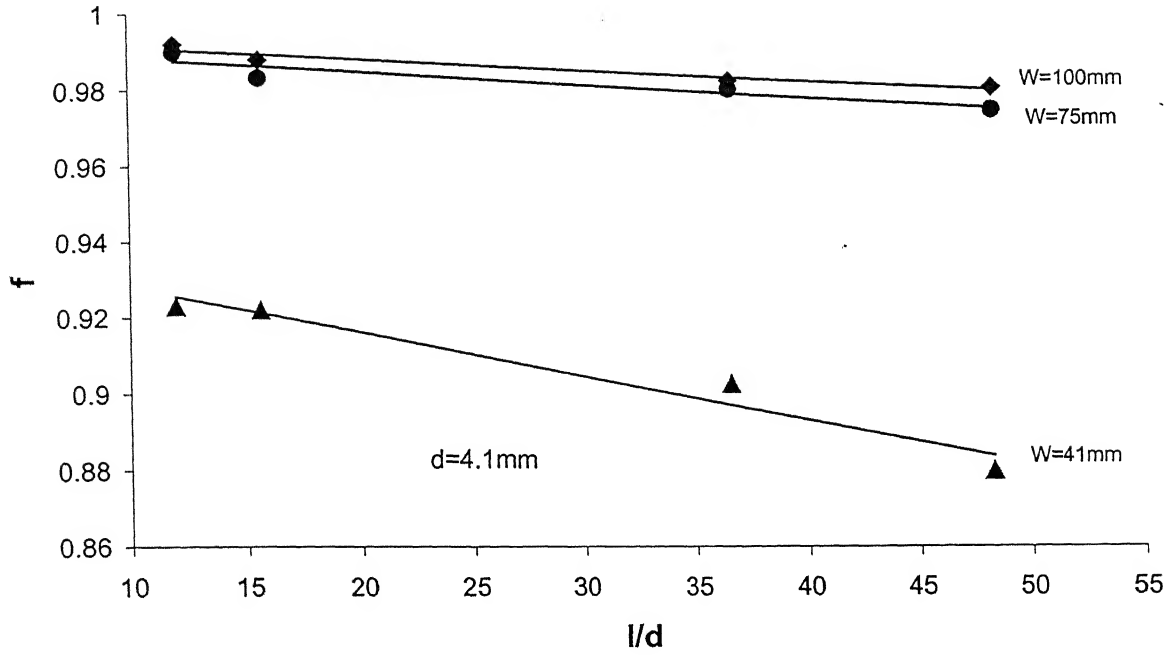

Fig. 4.15. Wall factor for long cylinders (l/d>10) falling vertically as a function of l/d.

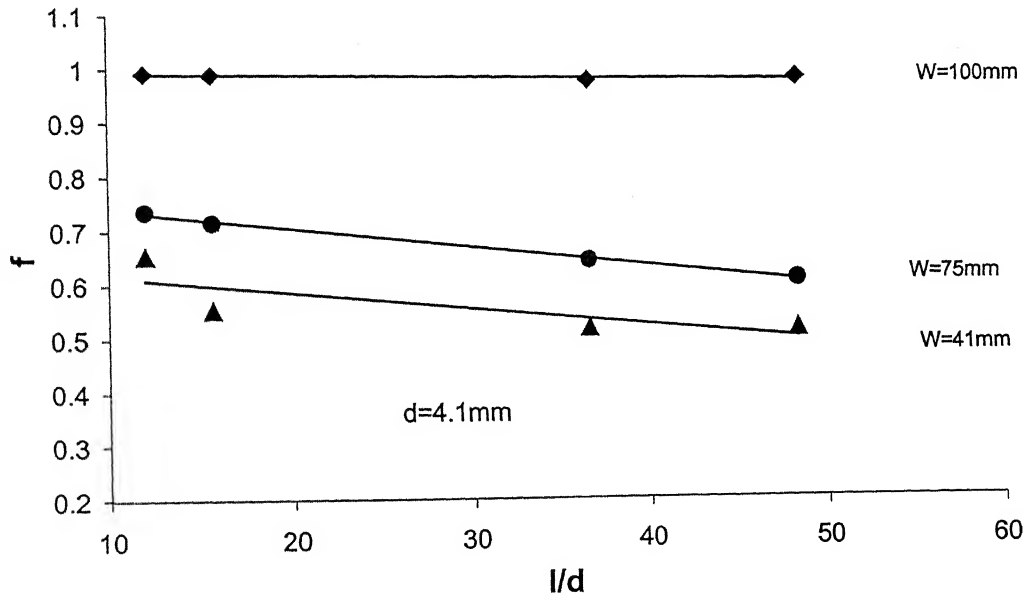

Fig. 4.16. Wall factor for long cylinders (l/d>10) falling horizontally as a function of l/d.

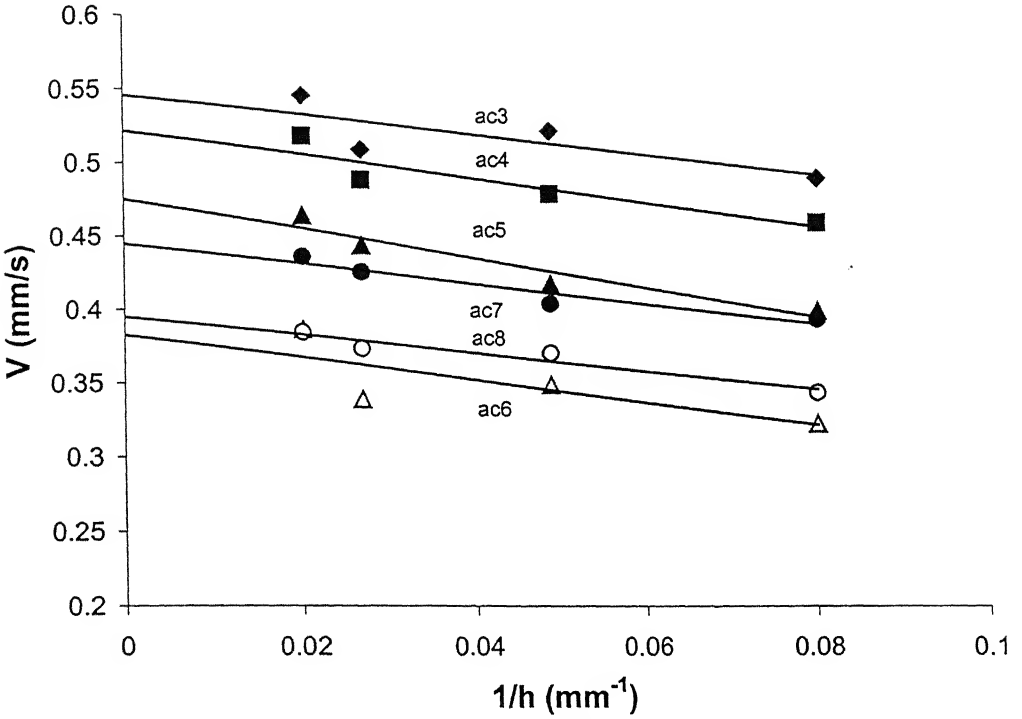

Fig. 4.17. Variation of settling velocity with width of the rectangular vessels in 3% CMC solution (vertical orientation).

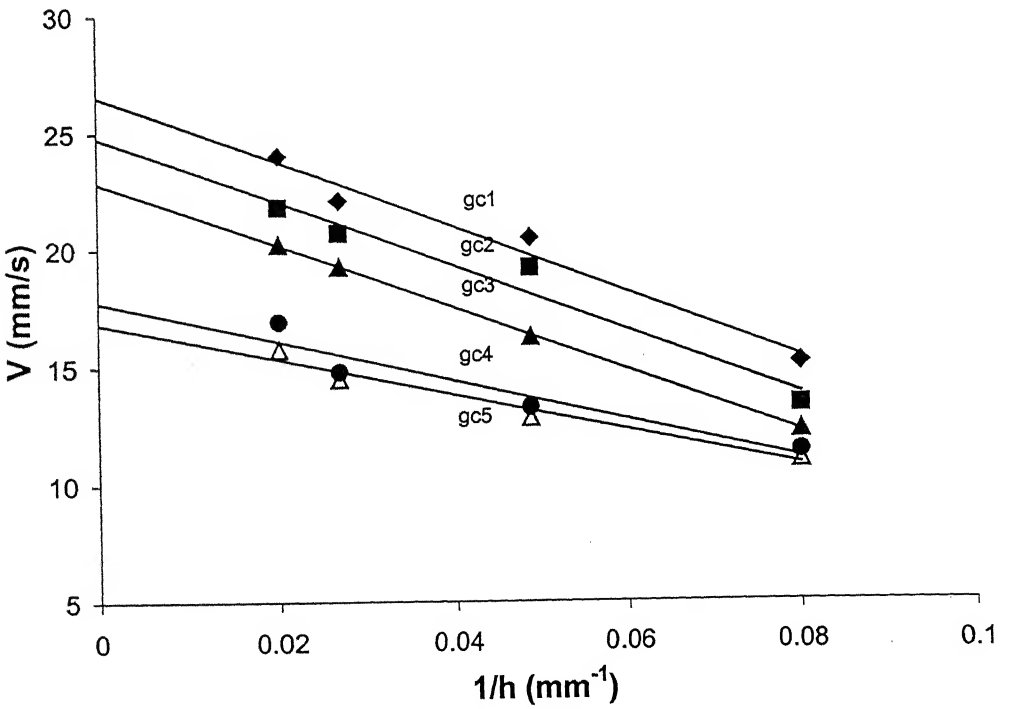

Fig. 4.18. Variation of settling velocity with width of rectangular vessels in 2% CMC solutions (vertical orientation).

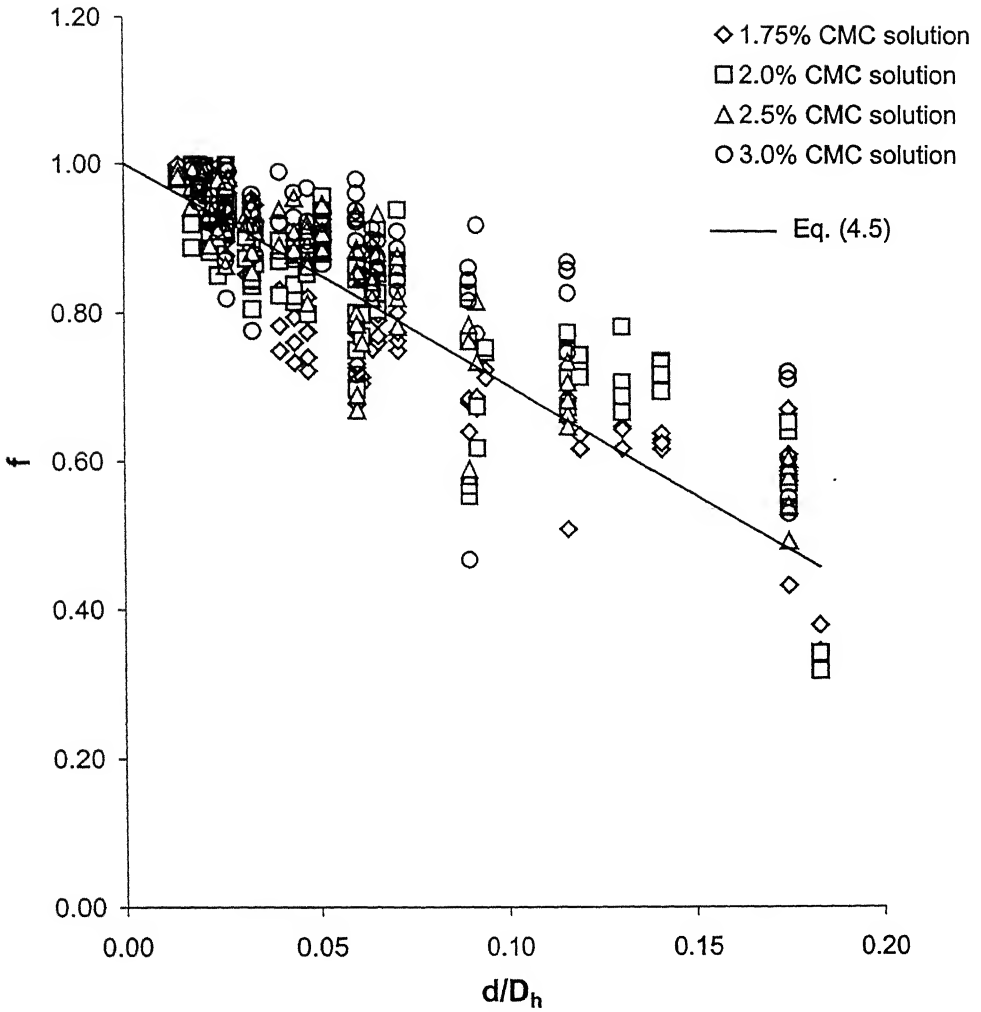

Fig. 4.19. Wall factor for cylinders falling vertically as a function of d/D_h (non-Newtonian media).

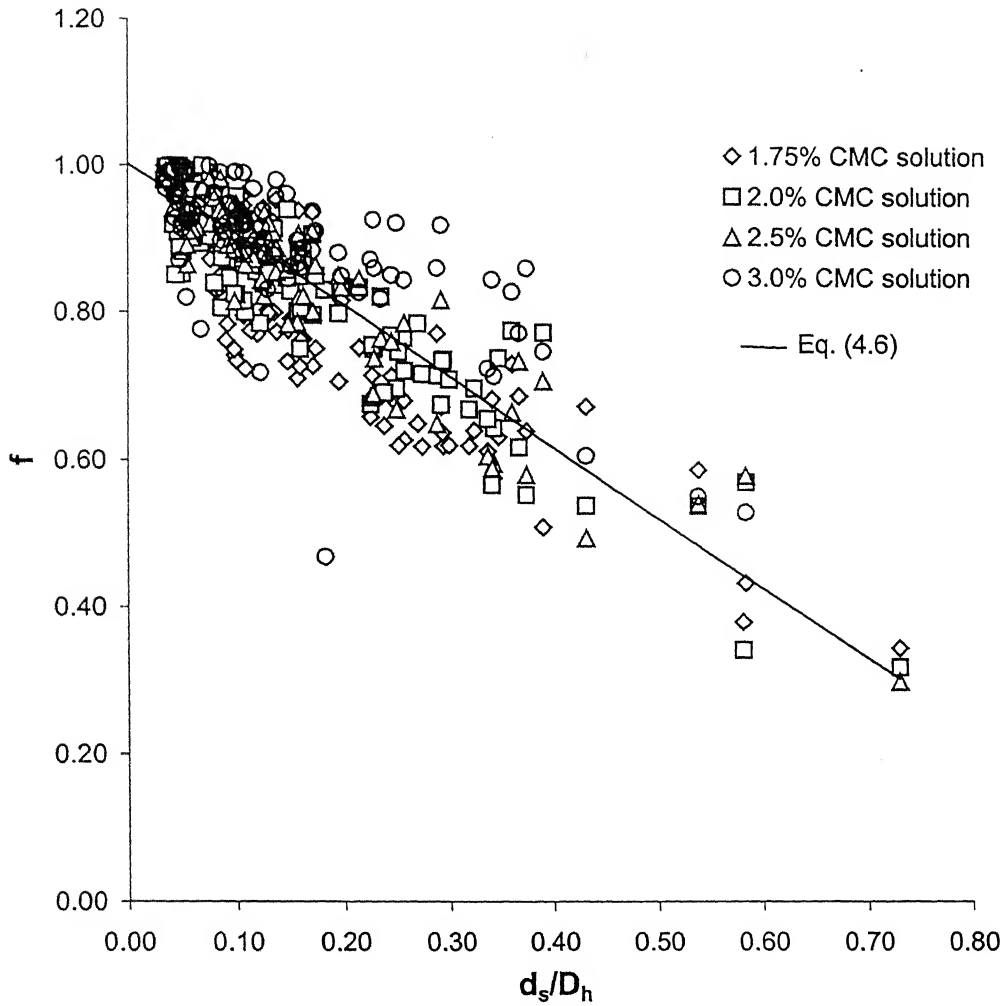

Fig. 4.20. Wall factor for cylinders falling vertically as a function of d_s/D_h (non-Newtonian media).

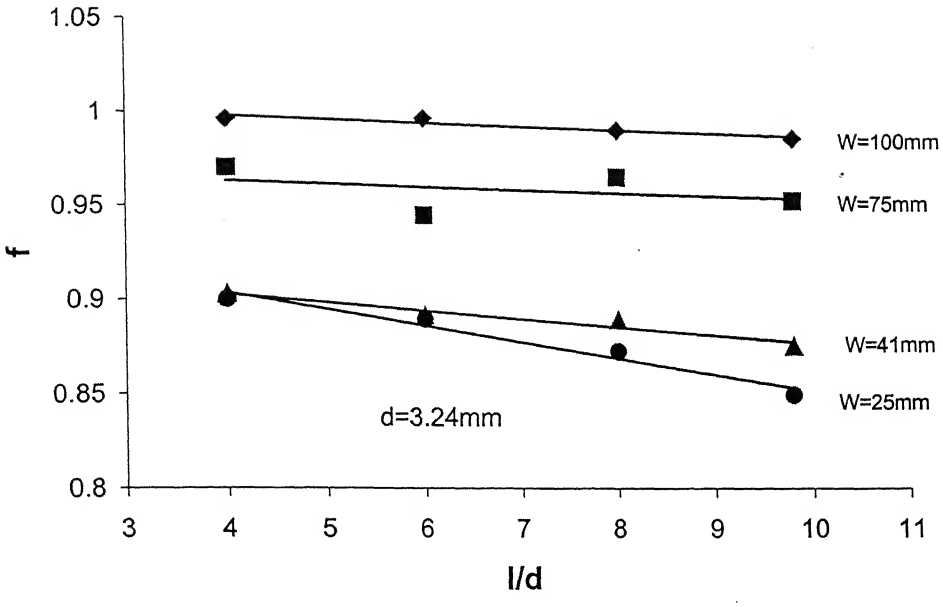

Fig. 4.21. Wall factor for short cylinders (l/d<10) falling vertically in CMC solutions as a function of l/d.

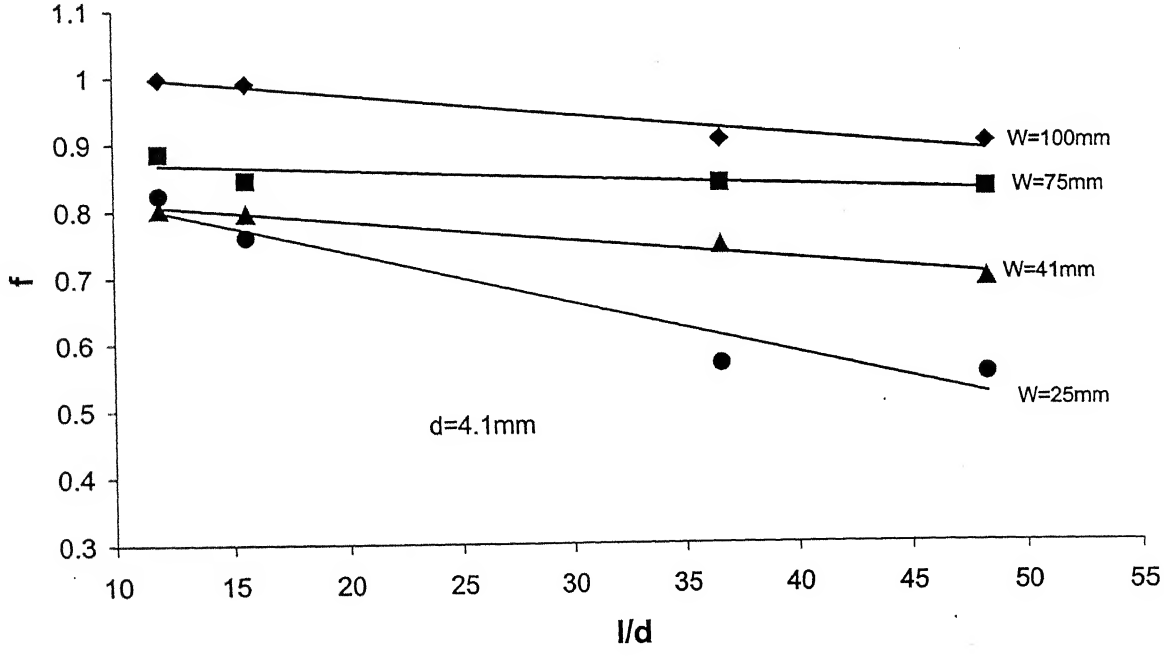

Fig. 4.22. Wall factor for long cylinders (l/d>10) falling vertically in CMC solutions as a function of l/d.

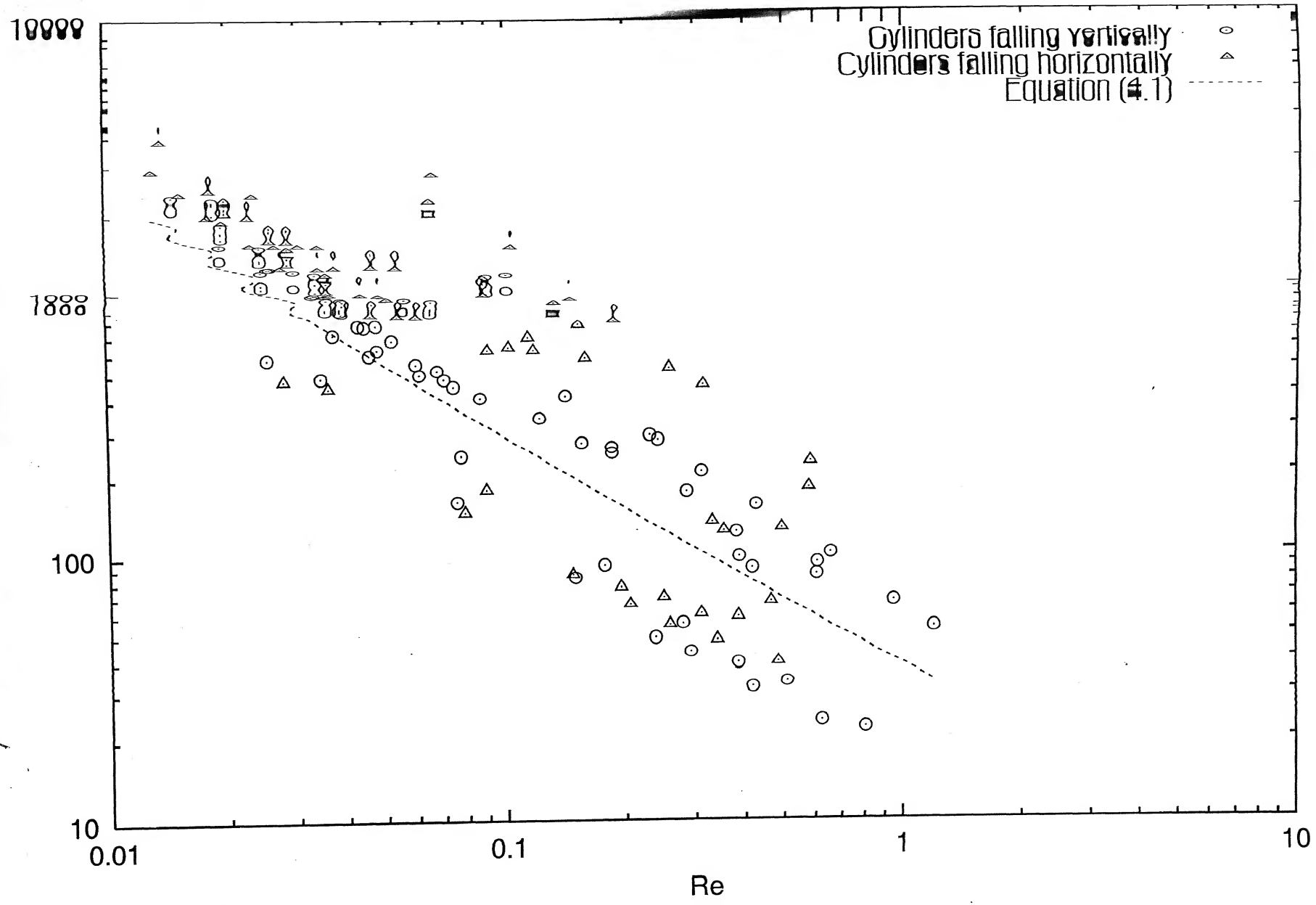

Fig. 4.23. Comparison of present drag results for cylinders with the literature (Newtonian media)

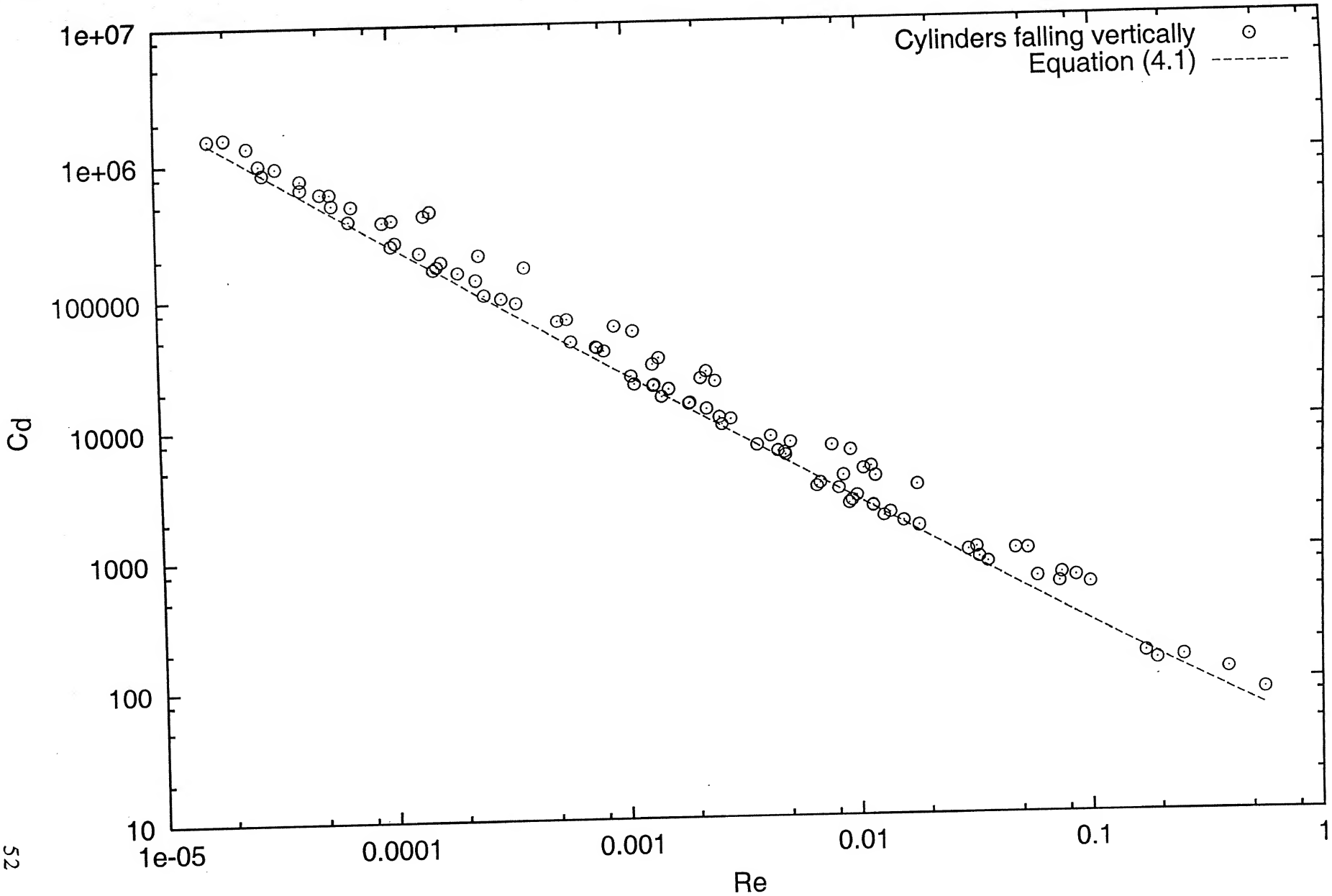

Fig. 4.24. Comparison of present drag results for cylinders with the literature (non-Newtonian media).

Chapter 5

Conclusions and Recommendations

Free settling velocity of a range of cylinders in several Newtonian and non-Newtonian fluids has been measured. Measurements were carried out in rectangular fall vessels of different width to assess the significance of possible wall effects. In this work, it has been found that the terminal settling velocity of cylindrical particles in otherwise stationary media is strongly influenced by the presence of bounding walls in both Newtonian and non-Newtonian fluids. The wall effect has been quantified in terms of a wall factor. The wall factor is correlated with the ratio of cylinder diameter-to-hydraulic diameter of fall vessel and equivalent volume diameter of cylinder-to hydraulic diameter of fall vessel for vertical as well as horizontal orientations for Newtonian fluids. For vertical orientation the correlation is linear whereas for horizontal orientation the data fitted to a quadratic equation. The scatter present in the wall factor results suggests that some additional parameter is needed to account for the shape of the particle, e.g., length-to-diameter ratio and/or sphericity. The present wall factor results for vertical orientation is compared with Venumadhav and Chhabra (1995), and it can be concluded that the presence of a rectangular boundary offers less wall resistance that of a circular boundary. For non-Newtonian fluids, the wall factor results are correlated in the same manner as for Newtonian fluids for vertical orientation (for cylinders in non-Newtonian media, the preferred orientation is vertical only). The present results are compared with that of Venumadhav and Chhabra (1995), and it is seen that the wall resistance is less in rectangular boundary than in circular one. Comparing the wall effect results for both fluids, it is concluded that the wall factor is less severe in case of non-Newtonian fluids than in Newtonian fluids. The influence of aspect ratio of cylinders on the extent of wall factor has been analyzed for $l/d<10$ and $l/d>10$. The slope of the line tends to decrease with increasing l/d ratio.

In the present study, both forms of representation of terminal velocity data (i.e.. drag coefficient-Reynolds number approach and velocity ratio approach) have been used. The drag results obtained for vertical and horizontal orientations are compared with the theoretical correlation of Venumadhav and Chhabra (1995) ($0.1<Re<423$, $n=1$). For Newtonian fluids, the agreement is not good as the Reynolds numbers for the present study are less than one and the experiments has been done for both orientations. Hence additional parameter like projected area (A_n) should come into picture. However, for non-Newtonian fluids the above correlation holds good. The effects of orientation and shape on the settling rates of individual cylinders were quantified in terms of K_∞. The experimental results were compared with the available literature. It is seen that, the free settling velocity is determined principally by the orientation, the sphericity and the d_s/d_n ratio of the particle.

5.1 Scope for Future work

Clearly, considerable scope exists for further theoretical and experimental works in this area. On the experimental front, the study can be extended to other confining wall as well as particle combination. Also some experimental work can be done for hindered settling of various shapes of particles in low as well as high Reynolds number region. Likewise, with the presently available levels of computational power, it should be possible to develop a theoretical structure to rationalize some of the experimental results presented herein.

References

Alger, G.R. and Simons, D.B., "Fall Velocity of Irregular Shaped Particles', J. Hydraulics Duvision (3), 721-737 (1968).

Balaramakrishnan, P.V., R.P. Chhabra, "Sedimentation of a Sphere Along the Axis of a Long Square Duct Filled with Non-Newtonian Liquids", Can. J. Chem Engg., 70, 803-807 (1992).

Bernhardt, "Sedimentation of Non-Spherical Particles", Part. Part. Syst., Charact., 8, 209-214 (1991).

Blumberg, P.N. and Mohr, M.C., "Effect of Orientation on the Settling Characteristics of Cylindrical Particles", AIChEJ, 11, 910-916 (1965).

Brenner, H. J. Fluid Mech. 12, 35 (1962).

Cheng Y.S., "Drag Forces on Non-Spherical Aerosol Particles", Chem. Engg Comm., 108, 201-223 (1991).

Chhabra, R.P., "Wall Effects on Terminal Velocity of Non-Spherical Particles in Non-Newtonian Polymer Solutions", Powder Technology 88, 39-44 (1996).

Chhabra, R.P., Encyclopedia of Fluid Mech., 7, 253-286 (1988).

Chhabra, R.P., "Wall Effects on Free-Settling Velocity of Non-Spherical Particles in Viscous Media in Cylindrical Tubes", Powder Technology 85, 83-90 (1995).

Chhabra, R.P., L. Agarwal, N.K. Sinha, "Drag on Non-Spherical Particles:An Evaluation of the Available Methods", Powder Technology 101, 288-295 (1999).

Chhabra, R.P. and P.H.T. Uhlherr, "The influence of Fluids Elasticity on Wall Effects for Creeping Motion in Cylindrical Tubes", Ca. J. Chem. Engg., 66, 154-157 (1988).

Chiba K., Song, K.W. and Horikawa, A., "Motion of a Slender body in Quiescent Polymer solutions", Rheol. Acta., 25, 380 (1986).

Cho, k., Cho, Y.I. and Park, N.A., 'Hydrodynamics of a vertically Falling Thin Cylinder in Non-Newtonian Fluids", J. Non-Newtonian Fluid Mech., 45, 105-145 (1992).

Cho, k., Pak, B. Cho, Y.I. and Park, N.A., 'Hydrodynamics of Large-Aspect Ratio Circular Cylinders Moving Vrtically in a Viscoelastic Fluids", ASME Winter Annual Meeting at Atlanta, December, 1991.

Christiansen, F.B. and Barker, D.H., "The Effect of Shape and Density on the Free Settling of Particles at High Reynplds Number", AIChEJ, 11, 145-147 (1965).

Clift R., J.R. Grace and M. e. Weber, "Bubbles, Drops and Particles, Academic Press, New York (1978).

Cox, R.G., "The Motion of Slender Rod-like Particles in a Second Order Fluids", J. Fluids Mech., 69, 305-307 (1975).

Faxen, H., "Die Bewegung einer Starren Kugel Langs der Achseeines mitzaher flussingkeit gefulltenrohes", Ask. Mat. Astron. Fys., 17, 1-28 (1923).

Finn, R.K., "Determination of the Drag on Cylinder at low Reynolds Number, J. Appl. Phys., 24, 771-773(1953).

Francis, A.W., Physics, 4, 403 (1933).

Haberman, W.L., and Sayre, R.M., "Motion of Rigid and Fluid Spheres in a Stationary and Moving Liquids inside Cylindrical Tubes", David Taylor Model basin, Report No. 1143, 1958.

Happel, J. and Brenner, "Low Reynolds Number Hydrodynamics", Prentice- Hall, Englewood Cliffs, New Jersey (1965).

Hasimoto, H., "Slow Motion of a Small sphere in a Cylindrical Domain", J. Phys. Soc. Jpn. 41, 2143-2144(1976).

Heiss, J.F. and J. Coull," The effect of Orientation and Shape on the Settling Velocity of Non-Isometric Particles in a Viscous Medium", Chem. Eng. Prog., 48, 133-140(1952).

Hetsroni-Handbook of Multiphase System, Hemisphere (1982).

Jayaweera K.O.l.F and Cottis R.E., "Fall Velocity of Plate-Like and Columnar Crystals" J.Roy. Met Soc., 95,703-709 (1969).

Johnson D.L., Leith, D. and Parker, C. R., "Drag on Non-Spherical, Orthrotropic Aerosol Particles", J. Aerosol Sci., 18, 87-97 (1987).

Jones, A.M. and Knudsen J.G., "Drag Coefficients at low Reynolds Number for Flow Past immersed Bodies", AICheJ, 7, 20-25 (1961).

Kasper G.,"Dynamics and Measurements of Smokes. I. Size Characterization of non-Spherical particles", Aerosol. Sci. Technol., 1, 187-19991982).

Kasper G., Niida T. and yang M., "Measurements of Viscous Drag on Cylinders and Chains of Spheres with aspect ratios Betweens 2 and 50" J. Aerosol. Sci., 16, 535-556 (1985).

Kasper G., "Wall Correction to the strokes Resistances of arbitrarily shaped particles", J. aerosol. Sci., 18, 457-459 (1987).

Kim S. and Karrila, S. J., "Micro hydrodynamics: Principles and Selected Application", Butterworths, Boston, 1991.

Leal, L.G., "Particles Motion in a Viscous Fluid", Ann.Rev. Fluid Mech., 44, 791-810 (1970).

Leal L.G., "The Slow Motion of Slender Rod Like Particles in a Second Order Fluids", J. Fluid Mech., 69, 305-317(1975).

Leith, D. "Drag on Non-Spherical Objects", Aerosol Sci., Techno., 6, 153-161 (1987).

List, R. and R.S. Schmeanauer, "Free fall Behaviour of Planer Snow Crystals, conical Graupel and Small hail", J. atm. Sci., 28, 110-115 (1971).

Manero, O., Mena, B. and de Varges, L., " A note on the Translation of a thin rod inside Cylinder", Rheol. Acta., 20,226 (1987).

Masliyah Jacob, H, and Epstein Norman, "Numerical Study of Steady Flow past Spheroids", j. fluids mech., 44,493-512 (1970).

McNown J.S. and Malika J., "Effect of Particle Shape on settling Velocity at low Reynolds Number", Trans. Amer. Geo. Union, 31 ,74-82 (1950).

Miyamura, a.S. Iwasaki and T. Ishii, "Experimental wall Correction Factors of a Single solid spheres in Triangular and Square cylinders, Parallel Plates", int. J. multiphase Flow 7, 41-46 (1981).

Pazwash, H. and Robertson, J.M., "Fluids Dynamics Considerations of Bottom Materials", J. Hyd. Div., Proc. A.S.C.E., 97,1317 (1971).

Pettyjohn, E.S. and Christiansen, E.B., " Effect of Particles Shape on Free settling rates of isometric Particles", Chem. Eng. Prog., 44, 157-172 91948).

Reynolds, P.A. Jones, T.E.R., " An Experimental study of the Settling Velocities of Single Particles in Non-Newtonian Fluids", Int. J. Minerals Proc, 25,47(1989).

Roos, F.W. and Willmarth, W.W., " Some experimental results on Spheres and Disk Drag", AIChel, 9, 285-291(1971).

Rosko A., "Experimental on Flow Past a Circular Cylinder at very High Reynolds number ", J. Fluid Mech., 10, 345-356 (1961).

Sharma, M.K., Chhabra, R.P., "An experimental Study of Free Fall of Cones in Newtonian and Non-Newtonian Media: drag Coefficients and wall Effects", Chem. Eng. Process, 30, 61 (1991).

Sharma, M. K., M.Tech. Thesis, I.I.T.Kanpur (1990).

Sheaffer W., "Drag on Modified Rectangular Prisms", J. Aerosol. Sci., 18, 11-16 (1987).

Singh, A.N. and Roychoudhury, K.C., "Study of the Effects of Orientation and shape on the settling velocity of Non-Isometric Particles", Chem. Eng. Sci., 24, 1185-1186 (1969).

Subrahmanyam, N.V. and Chhabra, R.P., "the Influence of Carrier Rheology on Drag Coefficients of Non-Spherical Particles and its Significances in Hydraulic Transport of Solids", Int. J. Bulk Solids handling, 10, 417 (1990).

Swamee, P.K. and Chandra Shekhar, P.O., "Drag coefficients and fall velocity of Non-Spherical Particles", J. Hydraulics Engg., 117,660-667 (1991).

Unnikrishna A. and Chhabra, R. P., "An Experiment Study of Motion of Cylinders in Newtonian Fluids: Wall Effects and Drag Coefficients", can. J. Chem. Eng., 69,729-735 (1991).

Unnikrishna A. and Chhabra, R.P., "Slow Parallel Motion of Cylinders in Non-Newtonian Media: wall Effects and Drag Coefficients", Chem. Eng. Process, 28,121 (1990).

Unnikrishna A., M.Tech. Thesis, I..I..T Kanpur (1990).

Venu Madhav, G., Chhabra, R.P., "Drag on Non-Spherical particles in Viscous Fluids", Int. J. Miner. Process. 43, 15-29 (1995).

Venu Madhav G., M. Tech. Thesis, I.I.T. Kanpur (1994).

Voryskaya L.P. and Taganov G.I., "Experimental study of the Drag of Circular Cylinders of High Aspect Ratio at Re <<1", Fluid Mechanics of Soviet Research,8, 53-59 (1979).

Willmarth, W. W.,Hawk, N.E. andHarvey, R.L., " steady and unsteady motion and wakes of Freely falling Disks", Phys. Fluids, 7, 197-208(1964).

Zheng, G., Powell, R.L., Stroeve, P., "Settling Velocity of a Sphere Between Two Concentric Cylinders Filled with a viscous Fluids". Ind. Eng. Chem. Res. 31, 1366-1372 (1992).

Nomenclature

A_p	Projected area of particle
B	Breadth of the rectangular vessel
C_d	Drag coefficient
d	Diameter of cylinder/sphere
d_n	Diameter of a circle having same area as the projected area of a non-spherical particle
d_s	Diameter of a sphere having same volume as that of a cylindrical particle
D	Diameter of cylindrical fall tube
D_h	Hydraulic diameter defined as four times the ratio of flow area to the wetted perimeter
f	Wall factor
F_D	Drag force on a particle
g	Acceleration due to gravity
h	Half width of rectangular channel
H	Height of rectangular channel
k	Power law consistency index
K_∞	Shape correction factor/Velocity ratio at infinite medium
l	Length of cylinder
n	Flow behavior index
Re	Particle Reynolds number
V	Terminal velocity of test particles
V_∞	Unbounded terminal velocity of test particles

$V_{s\infty}$ Free settling velocity of a sphere (diameter = d_s) in an infinite medium

W Width of rectangular channel (= 2h)

ρ_f Fluid density

ρ_p Particle density

Ψ Sphericity of cylindrical particle

APPENDIX A

Dimensions and Properties of Test Particles

Particle no.	*d, mm*	*Density, kg/m^3*
gs1	6.186	2186.64
gs2	4.730	2499.58
gs3	4.216	2663.27
gs4	4.000	2358.97
ss1	6.300	7943.52
ss2	4.720	7964.25
ss3	3.960	7983.99
ss4	3.180	8047.47

Particle no.	*d, mm*	*l, mm*	*d_s, mm*	*Density, kg/m^3*
gc1	8.000	199	26.73	2269.90
gc2	8.000	156	24.65	2270.67
gc3	8.000	80.0	19.73	2272.55
gc4	8.000	40.0	15.66	2273.82
gc5	8.000	38.0	15.39	2275.34
gc6	4.100	198	17.09	2268.77
gc7	4.100	150	15.58	2274.51
gc8	4.100	64.0	11.73	2276.12
gc9	4.100	49.0	10.73	2278.63
gc10	4.100	23.0	8.340	2280.10

Particle no.	*d, mm*	*l, mm*	*d_s, mm*	*Density, kg/m^3*
ac1	4.20	178	16.76	2689.35
ac2	4.20	90.0	13.35	2702.76
ac3	3.24	32.0	7.960	2695.40
ac4	3.24	26.0	7.425	2704.56
ac5	3.24	19.5	6.746	2713.79
ac6	3.24	13.0	5.893	2716.21
ac7	3.00	29.0	7.315	2703.13
ac8	3.00	24.0	6.868	2714.84
ac9	3.00	17.5	6.182	2722.09
ac10	3.00	12.0	5.451	2728.16
ac11	2.74	27.0	6.724	2719.36
ac12	2.74	22.0	6.280	2726.47
ac13	2.74	17.0	5.763	2731.52
ac14	2.16	30.0	5.943	2720.27
ac15	2.16	20.0	5.192	2727.45

Particle no.	*d, mm*	*l, mm*	*d_s, mm*	*Density, kg/m^3*
t1	8.08	50.0	16.98	1363.35
t2	8.08	30.0	14.32	1364.67
t3	8.08	20.0	12.51	1364.28
t4	8.08	15.0	11.36	1366.19
t5	8.08	10.0	9.930	1368.02
t6	8.08	5.00	7.881	1372.98
t7	8.08	2.0	5.806	1380.01

gs – Glass Sphere ss – Steel Sphere

gc – Glass Cylinder ac – Aluminium Cylinder

t – Teflon Cylinder

APPENDIX B

Wall Factor Data

Newtonian Media

87% glucose solution

	Vertical orientation		Horizontal orientation	
Particle no.	V_∞ *(m/s)*	f	V_∞ *(m/s)*	f
gc1	0.0478	0.97534	0.0228	0.98800
gc1	0.0478	0.81300	0.0228	0.53230
gc1	0.0478	0.49400	0.0228	0.33900
gc2	0.0479	0.86950	0.0203	0.98100
gc2	0.0479	0.62304	0.0203	0.57527
gc2	0.0479	0.43300	0.0203	0.39713
gc3	0.0374	0.88000	0.0150	0.75047
gc3	0.0374	0.77250	0.0150	0.98103
gc3	0.0374	0.56130	0.0150	0.75566
gc4	0.0229	0.92340	0.0141	0.63230
gc4	0.0229	0.94000	0.0141	0.71200
gc4	0.0229	0.87116	0.0141	0.60100
gc5	0.0233	0.89820	0.0148	0.59440
gc5	0.0233	0.97000	0.0148	0.70920
gc5	0.0233	0.77000	0.0148	0.62220
gc6	0.0114	0.98200	0.0075	0.98120
gc6	0.0114	0.97600	0.0075	0.60737
gc6	0.0114	0.88000	0.0075	0.51477
gc7	0.0111	0.98350	0.0081	0.97670
gc7	0.0111	0.98120	0.0081	0.64320
gc7	0.0111	0.90300	0.0081	0.51711
gc8	0.0107	0.98790	0.0088	0.98820
gc8	0.0107	0.98330	0.0088	0.71477
gc8	0.0107	0.92200	0.0088	0.55026
gc9	0.0108	0.93967	0.0084	0.96018
gc9	0.0108	0.98930	0.0084	0.73460
gc9	0.0108	0.92280	0.0084	0.65409
gc10	0.0091	0.99812	0.0084	0.96411
gc10	0.0091	0.90358	0.0084	0.81133
gc10	0.0091	0.92120	0.0084	0.63440
ac1	0.0279	0.98830	0.0120	0.99120
ac1	0.0279	0.72420	0.0120	0.61620

	Vertical orientation		Horizontal orientation	
Particle no	V_r *(m/s)*	f	V_∞ *(m/s)*	f
ac1	0.0279	0.68538	0.0120	0.50560
ac1	0.0279	0.36958	0.0120	0.19287
ac2	0.0205	0.91354	0.0128	0.99550
ac2	0.0205	0.90346	0.0128	0.70000
ac2	0.0205	0.82687	0.0128	0.55580
ac2	0.0205	0.46830	0.0128	0.19332
ac3	0.0116	0.98114	0.0083	0.99900
ac3	0.0116	0.85150	0.0083	0.74090
ac3	0.0116	0.82853	0.0083	0.67678
ac3	0.0116	0.51891	0.0083	0.32200
ac4	0.0112	0.97980	0.0080	0.92900
ac4	0.0112	0.86087	0.0080	0.81720
ac4	0.0112	0.78938	0.0080	0.76450
ac4	0.0112	0.50040	0.0080	0.35363
ac5	0.0094	0.96174	0.0076	0.93226
ac5	0.0094	0.88960	0.0076	0.82330
ac5	0.0094	0.81347	0.0076	0.77225
ac5	0.0094	0.52217	0.0076	0.36990
ac6	0.0081	0.96220	0.0065	0.98265
ac6	0.0081	0.88264	0.0065	0.84560
ac6	0.0081	0.86058	0.0065	0.77126
ac6	0.0081	0.54530	0.0065	0.47800
ac7	0.0102	0.99103	0.0075	0.98520
ac7	0.0102	0.84009	0.0075	0.74850
ac7	0.0102	0.79420	0.0075	0.68897
ac7	0.0102	0.55085	0.0075	0.31751
ac8	0.0093	0.97064	0.0073	0.97717
ac8	0.0093	0.88405	0.0073	0.83022
ac8	0.0093	0.81922	0.0073	0.68840
ac8	0.0093	0.53364	0.0073	0.60000
ac9	0.0080	0.97774	0.0072	0.99000
ac9	0.0080	0.88176	0.0072	0.74400
ac9	0.0080	0.84050	0.0072	0.68789
ac9	0.0080	0.55540	0.0072	0.35017
ac10	0.0069	0.94868	0.0055	0.96974
ac10	0.0069	0.92447	0.0055	0.87900
ac10	0.0069	0.86500	0.0055	0.80933
ac10	0.0069	0.57263	0.0055	0.52224
ac11	0.0085	0.97877	0.0066	0.98750

	Vertical orientation		Horizontal orientation	
Particle no.	V_∞ *(m/s)*	f	V_∞ *(m/s)*	f
ac11	0.0085	0.89235	0.0066	0.73320
ac11	0.0085	0.79737	0.0066	0.66320
ac11	0.0085	0.54233	0.0066	0.40265
ac12	0.0075	0.96364	0.0062	0.96700
ac12	0.0075	0.92422	0.0062	0.79283
ac12	0.0075	0.85258	0.0062	0.79916
ac12	0.0075	0.59022	0.0062	0.40670
ac13	0.0066	0.93935	0.0061	0.98205
ac13	0.0066	0.93480	0.0061	0.76757
ac13	0.0066	0.94543	0.0061	0.67099
ac13	0.0066	0.62320	0.0061	0.37122
ac14	0.0061	0.96076	0.0045	0.91604
ac14	0.0061	0.90900	0.0045	0.86930
ac14	0.0061	0.90190	0.0045	0.73400
ac14	0.0061	0.59852	0.0045	0.37220
ac15	0.0055	0.95885	0.0049	0.98710
ac15	0.0055	0.90448	0.0049	0.73146
ac15	0.0055	0.88164	0.0049	0.65850
ac15	0.0055	0.58003	0.0049	0.34860
86% glucose solution				
gc1	0.0664	0.91822	0.0323	0.86006
gc1	0.0664	0.78434	0.0323	0.77014
gc1	0.0664	0.66637	0.0323	0.38700
gc1	0.0664	0.49540	0.0323	0.29653
gc2	0.0569	0.90591	0.0347	0.85769
gc2	0.0569	0.78453	0.0347	0.76657
gc2	0.0569	0.74447	0.0347	0.41787
gc2	0.0569	0.50211	0.0347	0.29970
gc3	0.0453	0.92753	0.0370	0.86073
gc3	0.0453	0.89735	0.0370	0.75919
gc3	0.0453	0.84256	0.0370	0.51973
gc3	0.0453	0.70753	0.0370	0.32878
gc4	0.0392	0.88591	0.0333	0.88846
gc4	0.0392	0.93112	0.0333	0.76218
gc4	0.0392	0.82291	0.0333	0.60000
gc4	0.0392	0.67857	0.0333	0.40363
gc5	0.0372	0.87749	0.0317	0.88612

	Vertical orientation		Horizontal orientation	
Particle no.	V_∞ *(m/s)*	f	V_∞ *(m/s)*	f
gc5	0.0372	0.93838	0.0317	0.78864
gc5	0.0372	0.81900	0.0317	0.63858
gc5	0.0372	0.67568	0.0317	0.44306
gc6	0.0268	0.84030	0.0125	0.92166
gc6	0.0268	0.87590	0.0125	0.76480
gc6	0.0268	0.66869	0.0125	0.50000
gc6	0.0268	0.49347	0.0125	0.42400
gc7	0.0218	0.89243	0.0125	0.88106
gc7	0.0218	0.90656	0.0125	0.81968
gc7	0.0218	0.80760	0.0125	0.52980
gc7	0.0218	0.65531	0.0125	0.44640
gc8	0.0195	0.93241	0.0128	0.90000
gc8	0.0195	0.85487	0.0128	0.81719
gc8	0.0195	0.78174	0.0128	0.62500
gc8	0.0195	0.64587	0.0128	0.49765
gc9	0.0167	0.92126	0.0124	0.90613
gc9	0.0167	0.92982	0.0124	0.81790
gc9	0.0167	0.78174	0.0124	0.69355
gc9	0.0167	0.71976	0.0124	0.53336
gc10	0.0124	0.89597	0.0089	0.84225
gc10	0.0124	0.98920	0.0089	0.93320
gc10	0.0124	0.88234	0.0089	0.90753
gc10	0.0124	0.84357	0.0089	0.64873
ac1	0.0375	0.91323	0.0165	0.98990
ac1	0.0375	0.93240	0.0165	0.84406
ac1	0.0375	0.70547	0.0165	0.59420
ac1	0.0375	0.56980	0.0165	0.49515
ac1	0.0375	0.21798	0.0165	0.18773
ac2	0.0315	0.89676	0.0175	0.98760
ac2	0.0315	0.89175	0.0175	0.82102
ac2	0.0315	0.81819	0.0175	0.69514
ac2	0.0315	0.65079	0.0175	0.49686
ac2	0.0315	0.29854	0.0175	0.22006
ac3	0.0161	0.97050	0.0111	0.96874
ac3	0.0161	0.89280	0.0111	0.87802
ac3	0.0161	0.87500	0.0111	0.80294
ac3	0.0161	0.75850	0.0111	0.63622
ac3	0.0161	0.53188	0.0111	0.36306
ac4	0.0147	0.97503	0.0107	0.95365

	Vertical orientation		Horizontal orientation	
Particle no.	V_∞ *(m/s)*	*f*	V_∞ *(m/s)*	*f*
ac4	0.0147	0.89983	0.0107	0.88002
ac4	0.0147	0.85034	0.0107	0.84963
ac4	0.0147	0.75578	0.0107	0.63925
ac4	0.0147	0.52871	0.0107	0.40486
ac5	0.0133	0.97895	0.0101	0.95386
ac5	0.0133	0.94459	0.0101	0.90000
ac5	0.0133	0.83353	0.0101	0.83624
ac5	0.0133	0.80157	0.0101	0.68852
ac5	0.0133	0.60635	0.0101	0.44931
ac6	0.0114	0.96607	0.0088	0.95341
ac6	0.0114	0.96816	0.0088	0.89057
ac6	0.0114	0.83544	0.0088	0.91200
ac6	0.0114	0.79886	0.0088	0.77620
ac6	0.0114	0.61629	0.0088	0.53136
ac7	0.0136	0.96250	0.0097	0.97074
ac7	0.0136	0.94029	0.0097	0.88113
ac7	0.0136	0.82803	0.0097	0.79917
ac7	0.0136	0.80441	0.0097	0.65918
ac7	0.0136	0.57445	0.0097	0.38206
ac8	0.0128	0.93906	0.0093	0.96699
ac8	0.0128	0.93450	0.0093	0.90663
ac8	0.0128	0.88570	0.0093	0.80720
ac8	0.0128	0.81380	0.0093	0.65398
ac8	0.0128	0.59185	0.0093	0.41276
ac9	0.0114	0.91754	0.0085	0.98367
ac9	0.0114	0.97035	0.0085	0.90494
ac9	0.0114	0.89693	0.0085	0.83318
ac9	0.0114	0.81523	0.0085	0.72265
ac9	0.0114	0.61404	0.0085	0.49471
ac10	0.0100	0.91070	0.0074	0.97365
ac10	0.0100	0.87410	0.0074	0.91060
ac10	0.0100	0.98040	0.0074	0.82804
ac10	0.0100	0.86655	0.0074	0.79211
ac10	0.0100	0.59288	0.0074	0.52514
ac11	0.0114	0.99000	0.0082	0.97098
ac11	0.0114	9.96184	0.0082	0.93521
ac11	0.0114	0.77895	0.0082	0.78780
ac11	0.0114	0.79600	0.0082	0.67378
ac11	0.0114	0.59947	0.0082	0.43424

	Vertical orientation		Horizontal orientation	
Particle no.	V_∞ *(m/s)*	*f*	V_∞ *(m/s)*	*f*
ac12	0.0104	0.98721	0.0080	0.93000
ac12	0.0104	0.93353	0.0080	0.92188
ac12	0.0104	0.88211	0.0080	0.81370
ac12	0.0104	0.82183	0.0080	0.73788
ac12	0.0104	0.64808	0.0080	0.45100
ac13	0.0091	0.95556	0.0073	0.96603
ac13	0.0091	0.95725	0.0073	0.91447
ac13	0.0091	0.92500	0.0073	0.83325
ac13	0.0091	0.85714	0.0073	0.74288
ac13	0.0091	0.70593	0.0073	0.50959
ac14	0.0083	0.79313	0.0058	0.99776
ac14	0.0083	0.93108	0.0058	0.90362
ac14	0.0083	0.89639	0.0058	0.81724
ac14	0.0083	0.87687	0.0058	0.69186
ac14	0.0083	0.67048	0.0058	0.46483
ac15	0.0073	0.97429	0.0052	0.98315
ac15	0.0073	0.89534	0.0052	0.89615
ac15	0.0073	0.91082	0.0052	0.87972
ac15	0.0073	0.90356	0.0052	0.73288
ac15	0.0073	0.64315	0.0052	0.52448
82% glucose solution				
t1	0.0169	0.88580	0.0131	0.83336
t1	0.0169	0.90201	0.0131	0.81900
t1	0.0169	0.71633	0.0131	0.52720
t1	0.0169	0.61124	0.0131	0.36214
t2	0.0134	0.92590	0.0109	0.87376
t2	0.0134	0.86373	0.0109	0.85422
t2	0.0134	0.71642	0.0109	0.62000
t2	0.0134	0.62500	0.0109	0.50642
t3	0.0107	0.92168	0.0095	0.88755
t3	0.0107	0.89864	0.0095	0.85026
t3	0.0107	0.73365	0.0095	0.66537
t3	0.0107	0.65900	0.0095	0.54000
t4	0.0096	0.87980	0.0083	0.90410
t4	0.0096	0.86230	0.0083	0.89638
t4	0.0096	0.64615	0.0083	0.68200
t4	0.0096	0.53438	0.0083	0.60723

	Vertical orientation		Horizontal orientation	
Particle no.	V_∞ *(m/s)*	*f*	V_∞ *(m/s)*	*f*
t5	0.0069	0.96232	0.0068	0.88235
t5	0.0069	0.85754	0.0068	0.90221
t5	0.0069	0.80000	0.0068	0.73382
t5	0.0069	0.68884	0.0068	0.61882
t6	0.0044	0.91273	0.0046	0.96200
t6	0.0044	0.83932	0.0046	0.89609
t6	0.0044	0.85057	0.0046	0.81911
t6	0.0044	0.62000	0.0046	0.74044
t7	0.0021	0.98200	0.0022	0.98200
t7	0.0021	0.91750	0.0022	0.90000
t7	0.0021	0.95422	0.0022	0.93540
t7	0.0021	0.84230	0.0022	0.87091
80% glucose solution				
t1	0.0184	0.70310	0.0106	0.78360
t1	0.0184	0.62750	0.0106	0.52300
t1	0.0184	0.10400	0.0106	0.12840
t2	0.0138	0.72255	0.0104	0.76000
t2	0.0138	0.67160	0.0104	0.58000
t2	0.0138	0.17500	0.0104	0.15000
t3	0.0119	0.73780	0.0046	0.79300
t3	0.0119	0.66070	0.0046	0.62756
t3	0.0119	0.19440	0.0046	0.26400
t4	0.0095	0.73400	0.0085	0.81420
t4	0.0095	0.71220	0.0085	0.63600
t4	0.0095	0.23600	0.0085	0.29520
t5	0.0069	0.76220	0.0076	0.78140
t5	0.0069	0.76216	0.0076	0.64845
t5	0.0069	0.44270	0.0076	0.26700
t6	0.0038	0.76580	0.0044	0.84320
t6	0.0038	0.92870	0.0044	0.78900
t6	0.0038	0.52630	0.0044	0.49200
t7	0.0023	0.89400	0.0024	0.85050
t7	0.0023	0.80320	0.0024	0.79680
t7	0.0023	0.60510	0.0024	0.55225

Non-Newtonian Media

(Only for vertical orientation)

3.0% CMC solution

Particle no.	V_∞ *(m/s)*	f
gc1	0.00450	0.88462
gc1	0.00450	0.82856
gc1	0.00450	0.75067
gc1	0.00450	0.53367
gc2	0.00420	0.86706
gc2	0.00420	0.85033
gc2	0.00420	0.83200
gc2	0.00420	0.55524
gc3	0.00330	0.88040
gc3	0.00330	0.87758
gc3	0.00330	0.86285
gc3	0.00330	0.60972
gc4	0.00260	0.94038
gc4	0.00260	0.90077
gc4	0.00260	0.86154
gc4	0.00260	0.71677
gc5	0.00250	0.92080
gc5	0.00250	0.91532
gc5	0.00250	0.87322
gc5	0.00250	0.72672
gc6	0.00080	0.91990
gc6	0.00080	0.95903
gc6	0.00080	0.92413
gc6	0.00080	0.86433
gc7	0.00079	0.99176
gc7	0.00079	0.93792
gc7	0.00079	0.92815
gc7	0.00079	0.84785
gc8	0.00071	0.99861
gc8	0.00071	0.94859
gc8	0.00071	0.93870
gc8	0.00071	0.84600
gc9	0.00069	0.96437
gc9	0.00069	0.91657
gc9	0.00069	0.89804
gc9	0.00069	0.81957
gc10	0.00061	0.81933
gc10	0.00061	0.77600

Particle no.	V_∞ *(m/s)*	f
gc10	0.00061	0.71838
gc10	0.00061	0.46895
ac1	0.00150	0.99007
ac1	0.00150	0.87835
ac1	0.00150	0.85251
ac1	0.00150	0.77520
ac2	0.00120	0.99037
ac2	0.00120	0.91750
ac2	0.00120	0.88202
ac2	0.00120	0.92183
ac3	0.00054	0.99167
ac3	0.00054	0.94278
ac3	0.00054	0.96852
ac3	0.00054	0.91167
ac4	0.00052	0.99640
ac4	0.00052	0.93973
ac4	0.00052	0.92375
ac4	0.00052	0.88846
ac5	0.00047	0.95633
ac5	0.00047	0.93516
ac5	0.00047	0.88211
ac5	0.00047	0.84577
ac6	0.00039	0.99107
ac6	0.00039	0.86995
ac6	0.00039	0.89730
ac6	0.00039	0.83103
ac7	0.00046	0.94798
ac7	0.00046	0.92617
ac7	0.00046	0.88126
ac7	0.00046	0.86033
ac8	0.00040	0.96175
ac8	0.00040	0.93925
ac8	0.00040	0.92935
ac8	0.00040	0.86300
ac9	0.00037	0.97197
ac9	0.00037	0.91320
ac9	0.00037	0.90981
ac9	0.00037	0.87735
ac10	0.00028	0.96821
ac10	0.00028	0.92679
ac10	0.00028	0.96229
ac10	0.00028	0.89843

Particle no.	V_∞ *(m/s)*	f
ac11	0.00033	0.99374
ac11	0.00033	0.92461
ac11	0.00033	0.99036
ac11	0.00033	0.96204
ac12	0.00029	0.99215
ac12	0.00029	0.92067
ac12	0.00029	0.92158
ac12	0.00029	0.98090
2.5% CMC solution		
gc1	0.0098	0.91108
gc1	0.0098	0.84612
gc1	0.0098	0.71059
gc1	0.0098	0.58376
gc2	0.0096	0.90738
gc2	0.0096	0.83467
gc2	0.0096	0.66774
gc2	0.0096	0.54480
gc3	0.0091	0.88478
gc3	0.0091	0.82130
gc3	0.0091	0.65101
gc3	0.0091	0.49680
gc4	0.0067	0.94704
gc4	0.0067	0.82188
gc4	0.0067	0.73888
gc4	0.0067	0.59845
gc5	0.0064	0.94583
gc5	0.0064	0.84369
gc5	0.0064	0.68652
gc5	0.0064	0.60798
gc6	0.0023	0.91265
gc6	0.0023	0.85478
gc6	0.0023	0.67035
gc6	0.0023	0.58283
gc7	0.0021	0.93886
gc7	0.0021	0.88119
gc7	0.0021	0.69071
gc7	0.0021	0.59186
gc8	0.0017	0.97941
gc8	0.0017	0.94665
gc8	0.0017	0.80118
gc8	0.0017	0.78706

Particle no.	V_∞ *(m/s)*	f
gc9	0.0016	0.96970
gc9	0.0016	0.94430
gc9	0.0016	0.78630
gc9	0.0016	0.76545
ac1	0.0038	0.93784
ac1	0.0038	0.90932
ac1	0.0038	0.76145
ac1	0.0038	0.73714
ac2	0.0030	0.98153
ac2	0.0030	0.93370
ac2	0.0030	0.85077
ac2	0.0030	0.81900
ac3	0.0014	0.98882
ac3	0.0014	0.91479
ac3	0.0014	0.87193
ac3	0.0014	0.86436
ac4	0.0013	0.99121
ac4	0.0013	0.91242
ac4	0.0013	0.86358
ac4	0.0013	0.82215
ac5	0.0012	0.96700
ac5	0.0012	0.86358
ac5	0.0012	0.81400
ac5	0.0012	0.78392
ac6	0.0009	0.99038
ac6	0.0009	0.97622
ac6	0.0009	0.89289
ac6	0.0009	0.87780
ac7	0.0011	0.99231
ac7	0.0011	0.90027
ac7	0.0011	0.87920
ac7	0.0011	0.86282
ac8	0.0010	0.99004
ac8	0.0010	0.90980
ac8	0.0010	0.88560
ac8	0.0010	0.86700
ac9	0.0009	0.99578
ac9	0.0009	0.93344
ac9	0.0009	0.90878
ac9	0.0009	0.88300
ac10	0.0007	0.99206
ac10	0.0007	0.97814

Particle no.	V_∞ *(m/s)*	*f*
ac10	0.0007	0.95514
ac10	0.0007	0.93486
ac11	0.0009	0.96722
ac11	0.0009	0.89044
ac11	0.0009	0.88456
ac11	0.0009	0.85800
ac12	0.0008	0.99158
ac12	0.0008	0.93275
ac12	0.0008	0.89093
ac12	0.0008	0.88713
ac13	0.0007	0.99090
ac13	0.0007	0.94029
ac13	0.0007	0.93886
ac13	0.0007	0.93514
ac14	0.0005	0.99220
ac14	0.0005	0.96808
ac14	0.0005	0.93200
ac14	0.0005	0.92115
ac15	0.0005	0.98230
ac15	0.0005	0.94208
ac15	0.0005	0.91980
ac15	0.0005	0.91208
2.0% CMC solution		
gc1	0.0265	0.90711
gc1	0.0265	0.83486
gc1	0.0265	0.77645
gc1	0.0265	0.57525
gc2	0.0248	0.88040
gc2	0.0248	0.83654
gc2	0.0248	0.77843
gc2	0.0248	0.54198
gc3	0.0228	0.88785
gc3	0.0228	0.84869
gc3	0.0228	0.71667
gc3	0.0228	0.54148
gc4	0.0177	0.95763
gc4	0.0177	0.83824
gc4	0.0177	0.75311
gc4	0.0177	0.64642
gc5	0.0168	0.93887
gc5	0.0168	0.86518

Particle no.	V_∞ *(m/s)*	f
gc5	0.0168	0.67707
gc5	0.0168	0.65845
gc6	0.0068	0.90553
gc6	0.0068	0.83647
gc6	0.0068	0.69824
gc6	0.0068	0.55535
gc7	0.0062	0.90920
gc7	0.0062	0.84356
gc7	0.0062	0.75157
gc7	0.0062	0.56913
gc8	0.0052	0.99016
gc8	0.0052	0.84573
gc8	0.0052	0.79663
gc8	0.0052	0.76738
gc9	0.0047	0.99936
gc9	0.0047	0.80532
gc9	0.0047	0.80170
gc9	0.0047	0.82277
gc10	0.0037	0.99183
gc10	0.0037	0.89316
gc10	0.0037	0.78476
gc10	0.0037	0.83108
ac1	0.0107	0.92716
ac1	0.0107	0.91446
ac1	0.0107	0.76981
ac1	0.0107	0.62057
ac1	0.0107	0.32116
ac2	0.0088	0.94596
ac2	0.0088	0.86614
ac2	0.0088	0.79913
ac2	0.0088	0.67722
ac2	0.0088	0.34470
ac3	0.0040	0.98714
ac3	0.0040	0.95350
ac3	0.0040	0.87600
ac3	0.0040	0.85035
ac3	0.0040	0.74110
ac4	0.0038	0.99104
ac4	0.0038	0.96608
ac4	0.0038	0.79939
ac4	0.0038	0.87316
ac4	0.0038	0.69958

Particle no.	V_∞ *(m/s)*	f
ac5	0.0032	0.99731
ac5	0.0032	0.94525
ac5	0.0032	0.87241
ac5	0.0032	0.94069
ac5	0.0032	0.73791
ac6	0.0028	0.99679
ac6	0.0028	0.91482
ac6	0.0028	0.90279
ac6	0.0028	0.86896
ac6	0.0028	0.72221
ac7	0.0035	0.99903
ac7	0.0035	0.90189
ac7	0.0035	0.81543
ac7	0.0035	0.80574
ac7	0.0035	0.67114
ac8	0.0032	0.99813
ac8	0.0032	0.91056
ac8	0.0032	0.82366
ac8	0.0032	0.82891
ac8	0.0032	0.71131
ac9	0.0026	0.99927
ac9	0.0026	0.85092
ac9	0.0026	0.87335
ac9	0.0026	0.91446
ac9	0.0026	0.78681
ac10	0.0024	0.99792
ac10	0.0024	0.85000
ac10	0.0024	0.83875
ac10	0.0024	0.85488
ac10	0.0024	0.69271
ac11	0.0028	0.99938
ac11	0.0028	0.90567
ac11	0.0028	0.82403
ac11	0.0028	0.84671
ac11	0.0028	0.73664
ac12	0.0026	0.99463
ac12	0.0026	0.88173
ac12	0.0026	0.87058
ac12	0.0026	0.85662
ac12	0.0026	0.71823
ac13	0.0023	0.99719
ac13	0.0023	0.90770

Particle no.	V_∞ *(m/s)*	*f*
ac13	0.0023	0.89727
ac13	0.0023	0.86230
ac13	0.0023	0.74790
ac14	0.0018	0.98395
ac14	0.0018	0.88717
ac14	0.0018	0.87322
ac14	0.0018	0.85339
ac14	0.0018	0.75056
ac15	0.0016	0.97900
ac15	0.0016	0.91888
ac15	0.0016	0.90213
ac15	0.0016	0.86419
ac15	0.0016	0.75619
1.75% CMC solution		
gc1	0.0730	0.93696
gc1	0.0730	0.75267
gc1	0.0730	0.51114
gc1	0.0730	0.43624
gc2	0.0583	0.93913
gc2	0.0583	0.81681
gc2	0.0583	0.73302
gc2	0.0583	0.59146
gc3	0.0465	0.92695
gc3	0.0465	0.88865
gc3	0.0465	0.77357
gc3	0.0465	0.67627
gc4	0.0424	0.90019
gc4	0.0424	0.86709
gc4	0.0424	0.68962
gc4	0.0424	0.57807
gc5	0.0395	0.91066
gc5	0.0395	0.89142
gc5	0.0395	0.65928
gc5	0.0395	0.61448
gc6	0.0166	0.87583
gc6	0.0166	0.95318
gc6	0.0166	0.67839
gc6	0.0166	0.64223
gc7	0.0158	0.89648
gc7	0.0158	0.94183
gc7	0.0158	0.75346

Particle no.	V_∞ *(m/s)*	*f*
gc7	0.0158	0.68497
gc8	0.0135	0.91224
gc8	0.0135	0.92593
gc8	0.0135	0.72763
gc8	0.0135	0.68208
gc9	0.0132	0.92162
gc9	0.0132	0.91940
gc9	0.0132	0.71067
gc9	0.0132	0.68746
ac1	0.0259	0.96042
ac1	0.0259	0.92367
ac1	0.0259	0.71500
ac1	0.0259	0.68946
ac1	0.0259	0.34732
ac2	0.0229	0.97473
ac2	0.0229	0.94520
ac2	0.0229	0.70660
ac2	0.0229	0.67389
ac2	0.0229	0.38249
ac3	0.0106	0.99372
ac3	0.0106	0.99509
ac3	0.0106	0.77576
ac3	0.0106	0.75113
ac3	0.0106	0.63386
ac4	0.0098	0.99613
ac4	0.0098	0.99255
ac4	0.0098	0.72265
ac4	0.0098	0.76429
ac4	0.0098	0.64245
ac5	0.0089	0.99923
ac5	0.0089	0.99609
ac5	0.0089	0.74116
ac5	0.0089	0.77596
ac5	0.0089	0.62090
ac6	0.0074	0.98783
ac6	0.0074	0.96384
ac6	0.0074	0.82199
ac6	0.0074	0.80246
ac6	0.0074	0.62902
ac7	0.0090	0.99383
ac7	0.0090	0.99030
ac7	0.0090	0.79478

Particle no.	V_∞ *(m/s)*	f
ac7	0.0090	0.76208
ac7	0.0090	0.62131
ac8	0.0082	0.99916
ac8	0.0082	0.99633
ac8	0.0082	0.73376
ac8	0.0082	0.79189
ac8	0.0082	0.62167
ac9	0.0074	0.99937
ac9	0.0074	0.98640
ac9	0.0074	0.76100
ac9	0.0074	0.79961
ac9	0.0074	0.65125
ac10	0.0061	0.99410
ac10	0.0061	0.98282
ac10	0.0061	0.83046
ac10	0.0061	0.77036
ac10	0.0061	0.64752
ac11	0.0074	0.99953
ac11	0.0074	0.99077
ac11	0.0074	0.74908
ac11	0.0074	0.73300
ac11	0.0074	0.63943
ac12	0.0067	0.99847
ac12	0.0067	0.98452
ac12	0.0067	0.78300
ac12	0.0067	0.77333
ac12	0.0067	0.62000
ac13	0.0061	0.99959
ac13	0.0061	0.95200
ac13	0.0061	0.83131
ac13	0.0061	0.79043
ac13	0.0061	0.62095
ac14	0.0047	0.99610
ac14	0.0047	0.99145
ac14	0.0047	0.85174
ac14	0.0047	0.79867
ac14	0.0047	0.72676
ac15	0.0041	0.99913
ac15	0.0041	0.98606
ac15	0.0041	0.87107
ac15	0.0041	0.77479

APPENDIX C

Drag Coefficient – Reynolds Number Data

Newtonian Media

87% glucose solution

	Vertical orientation			Horizontal orientation		
Particle no.	V_∞ (m/s)	Re	C_d	V_∞ (m/s)	Re	C_d
gc1	0.04780	0.659051	101.0720	0.02281	0.31 44 97	4 48 .8499
gc2	0.04790	0.608989	92.81078	0.02030	0.25 81 78	5 16 .3901
gc3	0.03740	0.380600	121.8568	0.01500	0.15 26 47	7 57 .5483
gc4	0.02290	0.184966	257.9769	0.01410	0.11 38 87	6 80 .4772
gc5	0.02330	0.185012	244.9782	0.01480	0.11 75 18	6 07 .1 777
gc6	0.01143	0.100764	1130.219	0.00748	0.06 59 68	2 63 86 .961
gc7	0.01114	0.089573	1083.471	0.00806	0.06 48 05	2 03 89 .923
gc8	0.01076	0.065140	874.0964	0.00881	0.05 33 24	1 30 49 .376
gc9	0.01007	0.055778	912.7226	0.00837	0.04 63 36	1 32 22 .602
gc10	0.00907	0.039035	874.7994	0.00841	0.03 62 13	1 01 65 .438
ac1	0.02795	0.241629	275.4468	0.01198	0.10 36 11	1 49 83 .047
ac2	0.02049	0.141201	408.0125	0.01277	0.08 80 10	1 06 01 .222
ac3	0.01158	0.047536	761.5698	0.00831	0.03 41 07	1 41 90 .363
ac4	0.01119	0.042861	761.1777	0.00796	0.03 05 09	1 50 22 .254
ac5	0.00938	0.032653	983.5531	0.00764	0.02 65 85	1 41 33 .840
ac6	0.00806	0.024527	1162.049	0.00645	0.01 96 27	1 83 14 .689
ac7	0.01023	0.038626	896.1823	0.00756	0.02 85 25	1 65 43 .229
ac8	0.00933	0.033060	1012.531	0.00727	0.02 57 80	1 65 05 .148
ac9	0.00795	0.025360	1254.858	0.00725	0.02 31 34	1 50 07 .931
ac10	0.00689	0.019389	1471.666	0.00548	0.01 54 25	2 35 56 .370
ac11	0.00852	0.029578	1187.027	0.00657	0.02 28 01	1 99 97 .541
ac12	0.00750	0.024324	1429.957	0.00616	0.01 99 67	21 22 .080
ac13	0.00657	0.019557	1709.449	0.00608	0.01 80 97	1 99 96 .305
ac14	0.00606	0.018592	2074.300	0.00451	0.01 38 38	37 44 .540
ac15	0.00551	0.014775	2190.061	0.00490	0.01 31 44	27 67 .279

86% glucose solution

	Vertical orientation			Horizontal orientation		
Particle no.	V_∞ (m/s)	Re	C_d	V_∞ (m/s)	Re	C_d
gc1	0.06640	1.204402	52.94191	0.03230	0.585876	223.7334
gc2	0.05690	0.951696	66.48046	0.03470	0.580384	178.7556
gc3	0.04530	0.606468	83.95480	0.03700	0.495349	125.8457
gc4	0.03920	0.416538	88.98745	0.03330	0.353845	123.3140
gc5	0.03700	0.386507	98.19399	0.03170	0.331143	133.7734
gc6	0.02680	0.310818	207.7948	0.01250	0.144971	955.1780
gc7	0.02180	0.230477	286.2802	0.01250	0.132154	870.7315
gc8	0.01950	0.155203	269.3572	0.01280	0.101877	625.1409
gc9	0.01670	0.121596	335.9724	0.01240	0.090287	609.3870
gc10	0.01240	0.070168	473.5953	0.00890	0.050363	919.3287
ac1	0.03750	0.426491	154.3391	0.01650	0.187656	797.2064
ac2	0.03150	0.285448	174.2830	0.01750	0.158582	564.6768
ac3	0.01600	0.086392	402.5076	0.01110	0.059934	836.3116
ac4	0.01470	0.074066	444.9656	0.01070	0.053912	839.8342
ac5	0.01330	0.060884	493.8644	0.01010	0.046235	856.3835
ac6	0.01140	0.045587	587.2072	0.00880	0.035190	985.4527
ac7	0.01360	0.067508	512.1547	0.00970	0.048149	1006.782
ac8	0.01280	0.059655	542.8440	0.00930	0.043343	1028.322
ac9	0.01140	0.047823	616.0046	0.00850	0.035658	1108.041
ac10	0.01000	0.036990	705.8962	0.00740	0.027372	1289.073
ac11	0.01140	0.052016	670.0121	0.00820	0.037415	1294.985
ac12	0.01040	0.044320	751.8958	0.00800	0.034092	1270.704
ac13	0.00910	0.035587	901.2192	0.00730	0.028548	1400.450
ac14	0.00830	0.033473	1117.157	0.00580	0.023390	2287.781
ac15	0.00730	0.025719	1261.693	0.00520	0.018321	2486.524
82% glucose solution						
t1	0.01690	0.624362	23.44387	0.01310	0.483973	39.01756
t2	0.01340	0.417561	31.45279	0.01090	0.339658	47.53524
t3	0.01070	0.291265	43.09129	0.00950	0.258599	54.66507
t4	0.00960	0.237426	48.63718	0.00830	0.205275	65.06609
t5	0.00690	0.149077	82.24625	0.00680	0.146916	84.68304
t6	0.00440	0.075448	160.5244	0.00460	0.078877	146.8692
t7	0.00200	0.025265	572.3768	0.00220	0.027791	473.0388

80% glucose solution

	Vertical orientation			Horizontal orientation		
Particle no.	V_∞ (m/s)	Re	C_d	V_∞ (m/s)	Re	C_d
t1	0.01840	0.805978	22.04864	0.01060	0.464313	66.43635
t2	0.01380	0.509859	33.06171	0.01040	0.384242	58.21257
t3	0.01190	0.384067	38.83988	0.00960	0.309835	59.68007
t4	0.00950	0.278572	55.37050	0.00850	0.249248	69.16522
t5	0.00690	0.176753	91.69187	0.00760	0.194684	75.57912
t6	0.00380	0.077256	239.9352	0.00440	0.089454	178.9599
t7	0.00230	0.034449	482.5042	0.00240	0.035946	443.1332

Non-Newtonian Media (Vertical orientation only)

3.0% CMC solution

Particle no.	V_∞ (m/s)	Re	C_d
gc1	0.00450	0.002394	21363.02
gc2	0.00420	0.002072	22613.71
gc3	0.00330	0.001292	29320.13
gc4	0.00260	0.000805	37489.19
gc5	0.00250	0.000753	39862.11
gc6	0.00080	0.000148	432191.6
gc7	0.00079	0.000139	404019.2
gc8	0.00071	0.000102	376559.0
gc9	0.00069	0.000093	364756.0
gc10	0.00060	0.000067	374886.8
ac1	0.00150	0.000371	162700.0
ac2	0.00120	0:000237	202555.9
ac3	0.00054	0.000056	596046.0
ac4	0.00052	0:000051	599795.8
ac5	0.00047	0.000042	653092.2
ac6	0.00039	0.000029	846316.4
ac7	0.00046	0.000042	755124.4
ac8	0.00040	0.000033	937603.1
ac9	0.00037	0.000028	986312.7
ac10	0.00028	0.000017	1518589
ac11	0.00033	0.000025	1332499
ac12	0.00029	0.000020	1544699

2.5% CMC solution

Particle no.	V_∞ (m/s)	Re	C_d
gc1	0.00980	0.011193	4528.584
gc2	0.00960	0.010391	4351.659
gc3	0.00910	0.008511	3876.483
gc4	0.00670	0.004807	5675.839
gc5	0.00640	0.004456	6115.151
gc6	0.00230	0.001067	52568.72
gc7	0.00210	0.000889	57483.68
gc8	0.00170	0.000560	66035.70
gc9	0.00165	0.000511	64129.76
ac1	0.00380	0.002189	25471.88
ac2	0.00300	0.001371	32562.90
ac3	0.00140	0.000341	89098.28
ac4	0.00130	0.000295	96423.19
ac5	0.00120	0.000249	102815.2
ac6	0.00090	0.000152	159674.3
ac7	0.00110	0.000230	132680.4
ac8	0.00100	0.000193	150729.1
ac9	0.00090	0.000157	167490.9
ac10	0.00070	0.000101	244128.5
ac11	0.00090	0.000164	182186.5
ac12	0.00080	0.000133	215354.8
ac13	0.00070	0.000105	258129.1
ac14	0.00052	0.000069	482331.8
ac15	0.00048	0.000057	494545.7

2.0% CMC solution

gc1	0.02650	0.085075	622.4341
gc2	0.02480	0.073919	655.3366
gc3	0.02280	0.057989	620.6139
gc4	0.01770	0.035367	817.3417
gc5	0.01680	0.032470	891.9060
gc6	0.00680	0.009156	6044.158
gc7	0.00620	0.007611	6627.813
gc8	0.00520	0.005052	7093.171
gc9	0.00470	0.004154	7943.325
gc10	0.00370	0.002556	9960.856
ac1	0.01070	0.017577	3226.870
ac2	0.00880	0.011688	3801.204
ac3	0.00400	0.002794	10962.92

Particle no.	V_∞ (m/s)	Re	C_d
ac4	0.00380	0.002497	11335.01
ac5	0.00320	0.001845	14522.48
ac6	0.00280	0.001411	16570.10
ac7	0.00350	0.002197	13163.67
ac8	0.00320	0.001863	14784.89
ac9	0.00260	0.001299	20158.14
ac10	0.00240	0.001080	20859.93
ac11	0.00280	0.001515	18906.28
ac12	0.00260	0.001310	20479.00
ac13	0.00230	0.001046	24015.86
ac14	0.00180	0.000743	40432.31
ac15	0.00160	0.000582	44706.42
1.75% CMC solution			
gc1	0.07300	0.559961	82.24307
gc2	0.05830	0.388201	118.9024
gc3	0.04650	0.247467	149.6047
gc4	0.04240	0.189846	142.8165
gc5	0.03950	0.169984	161.7720
gc6	0.01660	0.052734	1016.945
gc7	0.01580	0.046593	1023.292
gc8	0.01350	0.031607	1055.212
gc9	0.01320	0.029075	1009.741
ac1	0.02590	0.098066	552.0477
ac2	0.02290	0.072174	562.6555
ac3	0.01060	0.017903	1564.810
ac4	0.00980	0.015385	1708.299
ac5	0.00890	0.012692	1881.862
ac6	0.00740	0.009030	2377.960
ac7	0.00900	0.013515	1995.516
ac8	0.00820	0.011416	2256.926
ac9	0.00740	0.009283	2494.369
ac10	0.00610	0.006559	3236.702
ac11	0.00740	0.009747	2713.225
ac12	0.00670	0.008136	3091.242
ac13	0.00610	0.006775	3422.325
ac14	0.00470	0.004762	5944.357
ac15	0.00410	0.003627	6824.473

APPENDIX D

Comparison of Experimental K_∞ values with that obtained from Equation 3.11 (Heiss and Coull, 1952).

Newtonian Media (for cylindrical particles in vertical orientation), Re < 1

d_s/d_n	ψ	l/d	K_∞ (Eq. 3.11)	K_∞^1	K_∞^2	K_∞^3
3.341	0.440	24.875	0.521303	0.164986	---	---
3.081	0.474	19.500	0.592983	0.635276	---	---
2.466	0.579	10.000	0.780427	0.627220	---	---
1.957	0.696	5.000	0.927294	1.203043	---	---
1.924	0.705	4.750	0.935890	0.798366	---	---
4.169	0.356	48.300	0.330760	0.356450	---	---
3.800	0.389	36.580	0.407385	0.392272	---	---
2.860	0.508	15.600	0.659108	---	---	---
2.617	0.550	11.950	0.733769	0.798319	---	---
2.034	0.677	5.600	0.907940	1.205130	---	---
3.990	0.371	42.400	0.365926	0.128282	---	---
3.180	0.461	21.400	0.565849	0.548690	---	---
2.456	0.581	9.800	0.783503	0.964456	0.898460	---
2.291	0.616	8.000	0.833999	0.764115	0.966986	---
2.082	0.665	6.000	0.894798	---	0.977665	---
2.438	0.585	9.670	0.789465	1.037590		---
2.289	0.616	8.000	0.834056	1.102229	1.294684	---
2.061	0.670	5.830	0.900359	0.744401	1.374664	---
1.817	0.733	4.000	0.959898	0.971218	0.893064	---
2.454	0.581	9.850	0.783611	0.756299	1.219982	---
2.292	0.616	8.000	0.833960	0.814416	0.859288	---
2.103	0.660	6.200	0.889112	0.879310	1.317458	---
2.751	0.526	13.800	0.692162	0.936670	1.150210	---
2.404	0.592	9.259	0.799953	---	1.369638	---
2.087	0.664	6.060	0.893667	0.793733	---	---
2.085	0.665	6.040	0.894230	0.790381	---	---
3.985	0.372	42.200	0.367755	0.369597	---	---
2.735	0.529	13.600	0.697434	0.853083	---	---
2.290	0.616	8.000	0.834035	1.060274	---	---
2.440	0.583	9.700	0.786870	0.878143	---	---
2.060	0.670	5.850	0.900360	1.330551	---	---
3.298	0.437	23.900	0.520055	0.341740	---	---
4.230	0.351	50.500	0.319146	0.175305	---	---

1.570	0.689	2.580	0.903870	0.787289	---	---
2.600	0.550	11.670	0.734902	---	0.550748	---
2.950	0.492	17.140	0.630009	---	0.452958	---
2.400	0.592	9.300	0.800132	---	0.556606	---
2.600	0.552	11.800	0.737958	---	0.529150	---
3.370	0.436	25.500	0.512961	---	0.405334	---
3.500	0.420	28.670	0.478242	---	0.417904	---
3.020	0.484	18.340	0.611948	---	0.483643	---
2.375	0.599	8.900	0.809707	---	0.866322	---
2.025	0.680	5.530	0.911134	---	1.379804	---
2.220	0.633	7.270	0.856289	---	1.471904	---
2.020	0.684	5.450	0.915397	---	2.066427	---
1.145	0.874	1.000	0.976249	---	---	0.949015
1.040	0.865	0.750	0.942074	---	---	0.966266
0.908	0.824	0.500	0.879712	---	---	0.992220
0.721	0.693	0.250	0.757918	---	---	0.783835
0.737	0.708	0.267	0.769381	---	---	0.738750
0.630	0.595	0.167	0.689431	---	---	0.870764
0.425	0.328	0.051	0.562980	---	---	0.429659
1.160	0.873	1.042	0.979574	---	---	0.755878
0.979	0.850	0.625	0.915468	---	---	0.808220
0.909	0.825	0.500	0.880373	---	---	0.781325
0.794	0.755	0.330	0.809196	---	---	0.694221
0.721	0.693	0.250	0.757918	---	---	0.643071

1 Data from M.Tech. Thesis (Kirti Rami, 2000, IIT Kanpur)

2 Data from M.Tech. Thesis (Venumadhav, 1995, IIT Kanpur)

3 Data from M.Tech. Thesis (Unnikrishnan, 1991, IIT Kanpur)

Non-Newtonian Media (Cylinders and Cones falling vertically), Re < 1

d_s/d_n	ψ	l/d^*	K_∞ (Eq. 3.11)	K_∞^1
1.817	0.733	4.000	0.959903	0.834273
1.738	0.755	3.500	0.976145	0.893313
1.666	0.774	3.080	0.987765	0.988372
1.554	0.800	2.500	0.998516	0.994172
1.442	0.820	2.000	0.999350	2.698145
1.640	0.780	2.940	0.990678	0.832871
1.554	0.801	2.500	0.999347	0.866496
1.442	0.826	2.000	1.003976	0.978857
1.440	0.830	2.000	1.006737	9.271523
1.310	0.858	1.500	1.003903	10.619470
1.440	0.830	2.000	1.006737	5.513308
1.360	0.858	1.670	1.013698	5.895691
1.310	0.858	1.500	1.003903	6.410256
1.430	0.836	1.950	1.009722	2.763385
1.278	0.858	1.460	0.997278	3.617270

d_s/d_n	ψ	l/d^*	K_∞ (Eq. 3.11)	K_∞^2
2.465	0.578	10.000	0.779223	0.114969
2.135	0.651	6.500	0.878663	0.146956
2.950	0.493	17.140	0.630905	0.179057
2.595	0.553	11.600	0.739165	0.208316
2.400	0.592	9.300	0.800132	0.222695
2.600	0.552	11.800	0.737526	0.202061
3.370	0.436	25.500	0.512961	0.171209
3.500	0.420	18.670	0.478242	0.180559
3.020	0.484	18.540	0.612372	0.174432
3.170	0.581	21.400	0.736013	0.283630
2.456	0.616	9.800	0.827269	0.319468
2.291	0.665	8.000	0.891895	0.382771
2.430	0.616	9.670	0.828433	0.263559
2.289	0.670	8.000	0.897761	0.213896
2.060	0.733	5.830	0.968063	0.284119
1.817	0.581	4.000	0.805243	0.362071
2.454	0.616	8.000	0.827360	0.361454
2.292	0.660	6.200	0.886031	0.338638
2.103	0.526	13.800	0.733831	0.435235
2.751	0.592	9.260	0.780325	0.318679

d_s/d_n	ψ	*Particle no.***	K_∞ *(Eq. 3.11)*	K_∞^3
0.859	0.834	c1	0.867989	2.326478
0.831	0.837	c2	0.859353	2.785516
0.707	0.797	c3	0.794513	1.910352
0.627	0.791	c4	0.757338	1.756955
0.617	0.766	c5	0.744460	2.089552
0.859	0.834	c1	0.867989	1.615911
0.831	0.837	c2	0.859353	1.814541
0.707	0.797	c3	0.794513	1.524990
0.627	0.791	c4	0.757338	1.506616
0.617	0.766	c5	0.744460	1.498501

1 Data from M.Tech. Thesis (Unnikrishnan, 1991, IIT Kanpur)

2 Data from M. Tech. Thesis (Venumadhav, 1995, IIT Kanpur)

3 Data from M. Tech. Thesis (M.K.Sharma, 1992, IIT Kanpur)

* Cylindrical Particles

** Cones